



1 **Secondary aerosol formation promotes water uptake**
2 **by organic-rich wildfire haze particles in Equatorial**
3 **Asia**

4 **Jing Chen^{1,*}, Sri Hapsari Budisulistiorini¹, Takuma Miyakawa², Yuichi Komazaki²,**
5 **Mikinori Kuwata^{1,3,4,*}**

6 [1] {Earth Observatory of Singapore, Nanyang Technological University, Singapore, Singapore}

7 [2] {Research and Development Center for Global Change, Japan Agency for Marine-Earth
8 Science and Technology, Yokosuka, Japan}

9 [3] {Asian School of Environment, Nanyang Technological University, Singapore, Singapore}

10 [4] {Campus for Research Excellence and Technological Enterprise (CREATE) program,
11 Singapore, Singapore}

12 * Correspondence to: chen.jing@ntu.edu.sg; kuwata@ntu.edu.sg

13

14

15

16

17

18

19

20



1 **Abstract**

2 Diameter growth factors (*GF*) of 100 nm haze particles at 85 % relative humidity and chemical
3 characteristics were simultaneously monitored at Singapore in October 2015 during a pervasive
4 wildfire haze episode, which was caused by peatland burning in Indonesia. Non-refractory
5 submicron particles (NR-PM₁) were dominated by organics (approximating 77.1 % in total mass),
6 whereas sulfate was the most abundant inorganic constituent (11.7 % on average). A statistical
7 analysis of the organic mass spectra showed that most of organics (36.0 % of NR-PM₁ mass)
8 were highly oxygenated. Diurnal variations of *GF*, number fraction of highly hygroscopic mode
9 particles, mass fraction of sulfate, and mass fraction of oxygenated organics (OOA)
10 synchronized well, peaking during daytime. The mean hygroscopicity parameter (κ) of haze
11 particles was 0.189 ± 0.087 , and mean κ values of organics were 0.157 ± 0.108 (κ_{org} , bulk
12 organics) and 0.287 ± 0.193 (κ_{OOA} , OOA), demonstrating the important roles of both sulfate and
13 highly oxygenated organics in hygroscopic growth of wildfire haze particles. κ_{org} was also
14 affected by the water-soluble organic fraction to some extent. These results show the importance
15 of secondary formation processes in promoting water uptake properties of wildfire haze particles,
16 including both inorganic and organic species. Further detailed size-resolved as well as molecular
17 level chemical information of organics will be necessary for more profound exploration of water
18 uptake by wildfire haze particles in Equatorial Asia.

19



1 1. Introduction

2 In the last few decades, wildfire haze has been periodically raging equatorial Asian
3 countries (Page et al., 2002; van der Werf et al., 2010; Field et al., 2016; Koplitz et al., 2016),
4 resulting in billions of dollars of economic losses as well as thousands of premature deaths
5 (Johnston et al., 2012; Marlier et al., 2013). The increasing wildfire activity is associated with
6 recent development of tropical peatland (Page et al., 2009; Spracklen et al., 2015). Water table
7 level of tropical peatland is artificially decreased by developing canals, enhancing flammability
8 of peat (Langner et al., 2007; Konecny et al., 2016). The occurrence of peatland fire is closely
9 related with El Niño-induced droughts (Page et al., 2002; Field et al., 2016). Enhanced peatland
10 fire has been observed during intense El Niño years, including 1997, 2006, and 2015 (Page et al.,
11 2002; van der Werf et al., 2010; Stockwell et al., 2016). The peatland fire in 1997 was globally
12 important, as the total carbon emission was estimated to equal 13–40 % of the year's annual
13 global carbon emission from fossil fuels (Page et al., 2002). The recent 2015 wildfire haze event
14 could rival the one in 1997 in terms of not only hazardous to human health but also the
15 significant impacts on global climate (Crippa et al., 2016; Field et al., 2016; Huijnen et al., 2016;
16 Koplitz et al., 2016; Stockwell et al., 2016). In fact, if there were a prize for the worst air
17 pollution disasters of the century, the 2015 equatorial Asian haze event would likely be
18 nominated (Crippa et al., 2016; Stockwell et al., 2016). During September – October 2015, the
19 thick smoke stemmed from peatland fires blanketed Equatorial Asia and released huge amounts
20 of organic material and fine particulate matter (particulate matters with the aerodynamic
21 diameter below 2.5 μm , $\text{PM}_{2.5}$) (Crippa et al., 2016; Koplitz et al., 2016), the leading cause of
22 global air-pollution-related mortality (Kunii et al., 2002; World Health Organization, 2009;
23 Johnston et al., 2012; Marlier et al., 2013; Lelieveld et al., 2015).

24 A previous study on the peatland fire event in 1997 has reported that the wildfire haze
25 particles resulted in dramatically cooling effects on the atmosphere radiative budget, especially
26 over the source region of Indonesia (-150 W m^{-2}) and the tropical Indian Ocean (-10 W m^{-2})
27 (Duncan et al., 2003). Along with the subsequently affected shallow warm clouds and deep
28 convection processes, the resultant abnormal rainfall in adjacent tropical region and extra-tropics
29 was also confirmed by both satellite observations and model simulations (Rosenfeld, 1999).
30 These studies demonstrate the importance of investigating aerosol-cloud-precipitation



1 interactions of Indonesian wildfire haze particles, including water uptake property of aerosol
2 particles.

3 Previous studies on water uptake properties of aerosol particles originating from
4 Indonesian peatland fire are controversial. Laboratory studies have demonstrated that fresh
5 Indonesian peat burning particles are weakly hygroscopic and almost inactive as cloud
6 condensation nuclei (CCN) (Chand et al., 2005; Dusek et al., 2005; Chen et al., 2017). On the
7 other hand, a field observation showed that the wildfire haze particles were highly hygroscopic
8 during the 1997 Indonesian peatland fires (Gras et al., 1999). The discrepancy impedes further
9 reliable evaluations on regional and global climate impacts driven by Indonesian wildfire haze
10 particles (Lin et al., 2013; Reid et al., 2013). The cause of the discrepancy will need to be
11 quantitatively understood in comparison with particle chemical composition.

12 Aerosol particles emitted from wildfire fire is a mixture of both inorganic and organic
13 compounds, complicating their water uptake properties (Carrico et al., 2008, 2010; Petters et al.,
14 2009; Hallar et al., 2013; Latham et al., 2013). Water uptake properties of inorganic salts such as
15 ammonium sulfate and ammonium nitrate are well known, yet hygroscopic behavior of organic
16 compounds or organic-inorganic mixtures are still difficult to predict due to the complex
17 chemical composition of organics and associated distinct affinity for water of a specific chemical
18 constitute (Saxena et al., 1995; Gysel et al., 2004; Dinar et al., 2007; Petters and Kreidenweis,
19 2007; Carrico et al., 2010; Kristensen et al., 2012; Marsh et al., 2017). For instance, experimental
20 and modelling studies have shown that water uptake by water-soluble matter is governed by the
21 inorganic fraction, whereas hygroscopic properties of inorganics can be altered substantially by
22 the presence of organics (Saxena et al., 1995; Dick et al., 2000). In general, with the increase of
23 organic fraction, water uptake by wildfire particles has performed an overall decreasing trend
24 (Mircea et al., 2005; Carrico et al., 2010), evidencing the high sensitivity of particle water uptake
25 to the organic fraction. The high sensitivity to organic fractions has been observed, as inorganic
26 species are much more hygroscopic than most of organic compounds. However, the roles of
27 inorganic and organic species in water uptake by Indonesian peatland burning particles have
28 rarely been investigated (Dusek et al., 2005; Chen et al., 2017).



1 Water uptake properties of organic compounds have also been demonstrated to be
2 important, especially when chemical composition of aerosol particles is dominated by organics.
3 Such cases are frequently observed for particles emitted from wildfires (Petters et al., 2009;
4 Carrico et al., 2010; Cubison et al., 2011; Hallar et al., 2013; Chen et al., 2017). Both theoretical
5 and experimental studies demonstrated that water-soluble organic matter (WSOM) plays the key
6 role in determining water uptake by organic compounds (Peng et al., 2001; Gysel et al., 2004;
7 Petters and Kreidenweis, 2007; Carrico et al., 2008; Petters et al., 2009; Lathem et al., 2013;
8 Chen et al., 2017). For instance, freshly emitted peat burning particles are known to contain a
9 small fraction of WSOM, explaining their limited hygroscopicity (Chen et al., 2017). Chemical
10 aging and oxidation of organic compounds both in gas and particle phases could alter water
11 uptake properties of aerosol particles in a wildfire plume (Gras et al., 1999; Petters et al., 2009;
12 Rose et al., 2010; Cubison et al., 2011). These chemical processes in the atmosphere enhance
13 fractions of highly oxygenated organics and polar species, which are typically water soluble
14 (Duplissy et al., 2008, 2011; Jimenez et al., 2009; Chang et al., 2010; Massoli et al., 2010;
15 Cubison et al., 2011; Cerully et al., 2015). Although such chemical transformation and
16 corresponding changes in hygroscopicity have been observed for wildfire particles both in
17 laboratory and field (Petters et al., 2009; Massoli et al., 2010; Rose et al., 2010; Cubison et al.,
18 2011; Duplissy et al., 2011), the importance of these processes on water uptake property has
19 never been investigated for peatland burning particles in equatorial Asian region.

20 In this work, we investigated the relationships between water uptake properties and
21 chemical composition of aerosol particles in tropical peatland fire haze in October 2015 by
22 conducting atmospheric observation in Singapore. We quantified water uptake properties using
23 the Humidified Tandem Differential Mobility Analyzer (HTDMA). In parallel, particle chemical
24 composition was characterized in real-time using the Aerodyne Time of Flight-Aerosol Chemical
25 Speciation Monitor (ToF-ACSM). Further, water-soluble organic carbon (WSOC) and elemental
26 carbon (EC) contents were quantified with off-line analysis using ambient PM_{2.5} filter samples.
27 The data from these measurements were combined to explore how water uptake property of
28 tropical peatland burning particles is regulated.

29



1 2. Observation

2 2.1. Field Campaign

3 The field observation was conducted at the campus of Nanyang Technological University
4 (NTU), Singapore (1°20'41" N, 103°40'53" E) during October 2015. The campus is located at
5 20 km away from the city center, and surrounded by a secondary tropical forest and grassland.
6 The site is located 0.8 km away from a highway, and a petrochemical complex (Jurong Island) is
7 located approximately around 8 km south.

8 The observation was performed in an air-conditioned room, with the room temperature
9 kept around 22 °C. A cyclone (URG-2000-30EN PM_{2.5}, URG) was employed for ambient
10 aerosol sampling at a flow rate of 16.67 L min⁻¹. The inlet was fixed on the rooftop, which is
11 located approximately 10 m above the ground. The sample air was split into several flows for
12 different instruments after drying by diffusion dryers (with the relative humidity, *RH*, of the
13 sample flow below 30 %). During the observation, particle number size distribution, chemical
14 composition, and hygroscopic growth were monitored.

15 2.2. Particle water uptake measurements

16 Water uptake property was measured using the HTDMA system (Chen et al., 2017).
17 Briefly, sampled particles were desiccated using a diffusion dryer (Model 42000, Brechtel
18 Manufacturing, Inc.), and resulting dry polydisperse particles were classified by the first
19 differential mobility analyzer (DMA, Model 3081, TSI Inc.). The DMA selects particles of a
20 specific mobility diameter (D_0), which was fixed at 100 nm during the observation. The
21 classified particles were humidified to $RH = 85\%$ using nafion tubings (MD-110-12S-4, Perma
22 Pure) operated under a controlled *RH* condition. The particle residence time in the humidifier
23 was approximately 10 seconds. The variation of *RH* was $\pm 0.5\%$ (peak to peak). The resulting
24 size distribution of humidified particles was measured by the second DMA coupled with a
25 condensation particle counter (CPC, Model 3775, TSI Inc.). The diameter growth factor
26 parameter, g , which is defined as the ratio of the particle diameter after humidification at a
27 conditioned *RH* ($D_p(RH)$) to the initial dry size (D_0) (i.e., $g = D_p(RH)/D_0$), was calculated from



1 the HTDMA data. Hygroscopicity parameter, κ , can be derived from the corresponding g at
2 given RH and D_0 using the following equation (Petters and Kreidenweis, 2007):

$$3 \quad \kappa = (g^3 - 1) \cdot \left(\frac{1}{RH} \cdot \exp\left(\frac{4\sigma_{s/a} \cdot M_w}{\rho_w \cdot R \cdot T \cdot D_0 \cdot g} \right) - 1 \right), \quad (1)$$

4 where $\sigma_{s/a}$ is the surface tension of the solution/air interface (0.0718 N m^{-1} at $25 \text{ }^\circ\text{C}$), M_w and ρ_w
5 are the molecular weight ($0.018 \text{ kg mol}^{-1}$) and density of water ($1 \times 10^3 \text{ kg m}^{-3}$), respectively, R
6 is the universal gas constant ($8.31 \text{ J K}^{-1} \text{ mol}^{-1}$), and T is absolute temperature (298 K). Further
7 details about the HTDMA are available in Chen et al. (2017).

8 **2.3. Aerosol chemical analysis**

9 The ToF-ACSM (Aerodyne Inc.) measured the chemical composition of non-refractory
10 submicron particles (NR-PM₁), including organics (OA), sulfate (SO₄²⁻), nitrate (NO₃⁻),
11 ammonium (NH₄⁺), and chloride (Cl⁻) (Fröhlich et al., 2013). The ToF-ACSM sampled particles
12 desiccated by a nafion tubing. The organic mass spectra measured by the ToF-ACSM were
13 analyzed in detail using a Multilinear Engine (ME-2 solver) software (Canonaco et al., 2013).
14 Four specific OA types were identified, i.e., hydrocarbon-like OA (HOA), peat burning OA
15 (PBOA), non-peat biomass burning OA (briefly, BBOA), and oxygenated OA (OOA). Details
16 about the ToF-ACSM measurements and data analysis are provided in Budisulistiorini et al. (in
17 preparation).

18 PM_{2.5} filter samples for chemical analysis were also collected using filter holders (BGI
19 Inc.). The samples were collected for 24 hours using 47 mm (diameter) quartz-fiber filters. The
20 sampling started/ended at 08:00 local time (LT). The collected samples were analyzed for bulk
21 OC, EC, and WSOC. All the quartz-fiber filters were prebaked at $900 \text{ }^\circ\text{C}$ for 3 hours before
22 sampling; after sampling, they were stored in a refrigerator ($-20 \text{ }^\circ\text{C}$) until analysis. For each
23 sampling, a back-up quartz-fiber filter was used to account for potential influence of gas phase
24 organic components on the particulate organics collected on the front quartz-fiber filter (Turpin
25 et al., 1994). The method assumes that all the particulate OC is collected by the front filter, while
26 gas phase OC is equally collected on both front and back filters. Subtraction of the OC loading



1 on the back filter (i.e., gas phase OC) from that on the front one allows quantification of
2 particulate OC (i.e., corrected OC).

3 Concentrations of OC and EC were determined by thermal-optical reflectance analysis
4 (Chow et al., 1993) using the Sunset Laboratory OC/EC Analyzer following the IMPROVE-A
5 protocol. WSOC was quantified with the Sievers 800 Total Organic Carbon (TOC) Analyzer
6 following extraction of a part of filter sample (8 mm ϕ) by 10 ml of HPLC-grade water. An
7 orbital shaker was operated for 21 hours for the extraction, and the subsequent solutions were
8 filtered with syringe filters (pore size of 0.2 μm).

9 **2.4. Particle number size distribution**

10 Particle number size distributions were measured using a NanoScan SMPS Nanoparticle
11 Sizer (NanoScan-SMPS, Model 3910, TSI Inc.) and an Optical Particle Sizer (OPS, Model 3330,
12 TSI Inc.). The detected particle size ranges are 11.5 – 365.2 nm (NanoScan-SMPS) in mobility
13 size and 0.3 – 10 μm (OPS) in aerodynamic size. Both the instruments sampled particles
14 desiccated by a diffusion dryer (Model 42000, Brechtel Manufacturing, Inc.). Time resolutions
15 of both the instruments were 1 minute.

16

17 **3. HTDMA data analysis**

18 **3.1. Classification of three hygroscopic modes**

19 Figure 1 shows the HTDMA data averaged over the whole observation period. The mean
20 normalized particle size distribution after humidification at 85 % *RH* has spanned a few different
21 modes, reflecting mixing states of ambient wildfire haze particles observed at Singapore
22 (Bougiatioti et al., 2016; Ogawa et al., 2016). For particles in a specific hygroscopic mode, *i*,
23 with $g_{1,i} < GF < g_{2,i}$, the number fraction of this mode (nf_i) can be derived from measured
24 probability density function of *g* (i.e., $c(g, D_0)$) as $nf_i = \int_{g_{1,i}}^{g_{2,i}} c(g, D_0) dg$. The corresponding



1 mean GF ($g_{mean,i}$) is calculated from $g_{mean,i} = \frac{1}{nf_i} \int_{g_{1,i}}^{g_{2,i}} g c(g, D_0) dg$ (Gysel et al., 2009). The
2 equivalent values of κ for mode i is obtained from $g_{mean,i}$ using Eq. (1).

3 Observed 100 nm dry particles were categorized into the following three groups based on
4 their hygroscopic properties at $RH = 85\%$, facilitating analysis of heterogeneity of particle
5 chemical composition.

6 (1) Nearly non-hygroscopic or weakly hygroscopic particles ($0 \leq \kappa < 0.1$; $g < 1.15$), those are
7 dominantly composed of black carbon (BC), non-polar hydrocarbon-like organic compounds
8 (Peng et al., 2001; Gysel et al., 2007; Kreidenweis et al., 2008);

9 (2) Moderately hygroscopic particles ($0.1 \leq \kappa < 0.2$; $1.15 \leq g < 1.27$), which could contain
10 hygroscopic organics (e.g., carboxylic acids and levoglucosan) and/or mixtures of non/less and
11 more hydrophilic compounds (e.g., BC, fatty acids, and/or humic-like substances mixed with
12 ammonium sulfate or levoglucosan-like species) (Peng et al., 2001; Chan and Chan., 2003; Gysel
13 et al., 2004, 2007; Chan et al., 2005; Petters and Kreidenweis, 2007);

14 (3) Highly hygroscopic particles ($\kappa \geq 0.2$; $g \geq 1.27$), those contain inorganic salts as well as some
15 highly hygroscopic organic species such as multifunctional organic acids (Peng et al., 2001;
16 Carrico et al., 2008; Duplissy et al., 2011; Ogawa et al., 2016).

17 In addition, a volume-weighted mean growth factor, GF , was also calculated using $c(g,$
18 $D_0)$ (Gysel et al., 2009):

$$19 \quad GF = \left(\int_0^{\infty} g^3 \cdot c(g, D_0) \cdot dg \right)^{1/3}. \quad (2)$$

20 GF was employed for calculating mean values of κ , facilitating comparison with chemical
21 composition of aerosol particles.

22 3.2. Effective κ of organic compounds (κ_{org})

23 Water uptake properties of organic compounds were estimated using the Zdanovskii-
24 Stokes-Robinson (ZSR) mixing rule, employing observed values of κ and chemical composition



1 as input parameters. The ZSR mixing rule assumes that water uptake by a mixture of materials is
 2 additive of water content retained by each chemical species (Stokes and Robinson, 1966). The
 3 rule also assumes that the volume change of the mixing of species within individual particles is
 4 almost negligible (Brechtel and Kreidenweis, 2000, Gysel et al., 2007; Petters and Kreidenweis,
 5 2007):

$$\begin{aligned}
 \kappa &= \sum_i \kappa_i \cdot \varepsilon_i = \kappa_{SNA} \cdot \varepsilon_{SNA} + \kappa_{org} \cdot \varepsilon_{org} + \kappa_{EC} \cdot \varepsilon_{EC} \\
 \Leftrightarrow \kappa_{org} &= \frac{\kappa - \kappa_{SNA} \cdot \varepsilon_{SNA} - \kappa_{EC} \cdot \varepsilon_{EC}}{\varepsilon_{org}}, \quad (3)
 \end{aligned}$$

7 where κ_i and ε_i stand for the hygroscopicity parameter and volume fraction of a specific
 8 component i in dry particles, respectively. The subscript SNA represents three major inorganic
 9 salts including sulfate, nitrate, and ammonium; org denotes organic species; EC indicates
 10 elemental carbon.

11 Sulfate, ammonium, and nitrate were considered for inorganics, the majority of which is
 12 contributed by sulfate (see Table 2). Other materials such as crustal elements were neglected
 13 because they are scarce for submicron wildfire haze particles in Southeast Asia
 14 (Balasubramanian et al., 2003; Keywood et al., 2003; Stockwell et al., 2016). Both sulfate and
 15 nitrate were almost completely neutralized by ammonia, and these three most abundant inorganic
 16 constituents were combined together and assumed as ammonium sulfate (i.e., $\varepsilon_{SNA} = \varepsilon_{SO_4} + \varepsilon_{NO_3} +$
 17 $\varepsilon_{NH_4} \approx \varepsilon_{AS}$). Thus the value of κ_{SNA} was considered as approximating the κ value of ammonium
 18 sulfate under the condition when sulfate dominates inorganics (Gunthe et al., 2009; Chang et al.,
 19 2010; Ogawa et al., 2016). The elemental carbon (EC) is known as non-hygroscopic (i.e., $\kappa_{EC} \approx$
 20 0).

21 Values of densities are required to compute ε_i from observed mass fractions. The mass
 22 fraction is taken as the first-order approximation of the volume fraction based on the hypothesis
 23 that the bulk particle density is similar to the densities of individual compounds assuming
 24 volume additivity (Kreidenweis et al., 2008; Gunthe et al., 2009; Hallquist et al., 2009). This
 25 hypothesis is demonstrated to be acceptable when particles are composed primarily of organics
 26 and sulfate (Cross et al., 2007; King et al., 2007). Densities of ammonium sulfate and EC were
 27 assumed as 1.77 g cm^{-3} and 1.80 g cm^{-3} , respectively (Park et al., 2004; Bond and Bergstrom,



1 2006). Density of organics is known to vary, depending on its elemental composition (Kuwata et
2 al., 2012). The value was assumed as 1.40 g cm^{-3} , which is a typical value for ambient organic
3 aerosols (Hallquist et al., 2009).

4 EC mass fraction of approximating 10.0 % in submicron wildfire haze particles was
5 simply utilized according to the time-averaged EC content in ambient $\text{PM}_{2.5}$ filter samples (see
6 Table 2). This assumption is on the basis of the preconditions that wildfire haze particles are
7 homogeneously mixed among different sizes and that there is no significant difference between
8 BC and EC.

9 3.3. κ of oxygenated organic compounds (κ_{OOA})

10 As described in Sect. 2.3, organics were numerically segregated to HOA, PBOA, BBOA,
11 and OOA. The value of κ_{org} can be calculated by a linear combination of contributions from
12 segregated fractions (Petters and Kreidenweis, 2007; Chang et al., 2010);

$$13 \kappa_{\text{org}} = v_{\text{HOA}} \cdot \kappa_{\text{HOA}} + v_{\text{PBOA}} \cdot \kappa_{\text{PBOA}} + v_{\text{BBOA}} \cdot \kappa_{\text{BBOA}} + v_{\text{OOA}} \cdot \kappa_{\text{OOA}}, \quad (4)$$

14 where v_i stands for the volume fraction of component i in the whole organics.

15 Both hydrocarbon (-like) and peat burning OA are known to be almost non-hygroscopic,
16 meaning that their κ values could be assumed as 0 (Gysel et al., 2007; Gunthe et al., 2009; Chang,
17 et al., 2010; Chen et al., 2017). Water uptake by freshly emitted biomass burning particles is
18 generally limited, especially compared with OOA (Carrico et al., 2010; Chang et al., 2010; Chen
19 et al., 2017). Water uptake by a mixed particle is largely driven by the relative abundance of
20 more and less hygroscopic components, and is more sensitive to uncertainties in hygroscopicity
21 of more hygroscopic compounds than that of less hygroscopic compounds (Gysel et al., 2007).
22 Thus, κ_{BBOA} was also assumed to be 0, considering that OOA always dominated over BBOA in
23 wildfire haze particles as suggested by our ToF-ACSM results (see Sect.4.2 and Fig. 6d). Under
24 these assumptions, κ_{OOA} can be calculated by the following equation:

$$25 \kappa_{\text{OOA}} = \kappa_{\text{org}} / v_{\text{OOA}}. \quad (5)$$



1 Density of OOA is required to calculate ν_{OOA} using ME-2 resolved OOA mass
2 concentration combined with total volume concentration of bulk OA derived from ToF-ACSM
3 observed OA mass. The density of oxygenated organics was assumed to be 1.50 g cm^{-3} (as
4 summarized in Table 1), which is appropriate typical value for carboxylic and multifunctional
5 organic acids (Saxena et al., 1995; Peng et al., 2001; Gysel et al., 2004; Carrico et al., 2010;
6 Ogawa et al., 2016). Detailed information on parameters utilized for the κ_{org} calculation is
7 provided in Table 1.

8

9 **4. Results**

10 In this section, aerosol number size distribution (Figure 2), chemical composition
11 (Figures 3 and 4), and hygroscopic properties of aerosol particles (Figure 5) are shown, in
12 addition to diurnal variation of these data (Figure 6).

13 **4.1 Number size distribution of wildfire haze particles**

14 Figure 2a displays the time averaged particle size distribution within the whole size range
15 of $11.5 \text{ nm} - 10 \text{ }\mu\text{m}$ measured by NanoScan-SMPS combined with OPS. The NanoScan-SMPS
16 data were used for the fine particles ($11.5 - 365.2 \text{ nm}$), and the overlapped size range of the OPS
17 (338 nm size bin) was excluded from the analysis. The data in the remaining OPS size range
18 ($419 \text{ nm} - 10 \text{ }\mu\text{m}$) were combined with the fine particle data. The temporal average size
19 distribution presents a unimodal structure with the number mode diameter located around
20 100 nm . Particles in the range of $30 - 200 \text{ nm}$ dominate the total particle number concentration
21 whereas particles larger than 600 nm only account for a minor fraction (less than 4.0% on
22 average), suggesting that wildfire haze particles in Singapore are predominantly contributed by
23 submicron particles.

24 Figure 2b shows the diurnal cycle of number size distribution. Particle number
25 concentrations (*i.e.*, dN/dlogD_p) higher than $1.5 \times 10^4 \text{ cm}^{-3}$ are commonly observed in the $50 -$
26 200 nm particle size range, while the number concentrations of super micron particles seldom
27 exceed $1.0 \times 10^3 \text{ cm}^{-3}$. Particle number concentration was high in the morning of $08:00 -$
28 $09:00 \text{ LT}$. The concentration increased again after noontime (about $14:00 \text{ LT}$), lasting until



1 midnight. The high concentration periods could be caused by local traffic emissions and by
2 secondary formation. The diurnal variation was also observed for number concentration of whole
3 particles.

4 Figure 2c depicts the mean diurnal variations of the corresponding total particle number
5 and volume concentrations. The total number concentration started to increase after 07:00 LT
6 until around 10:00 LT, and reached the highest level after 14:00 LT. The particle number
7 concentration was higher than $1.5 \times 10^4 \text{ cm}^{-3}$ before 19:00 LT. After that, the number
8 concentration decreased gradually, reaching $1.2 \times 10^4 \text{ cm}^{-3}$ in the midnight. Correspondingly, the
9 aerosol volume concentration was higher than $50.0 \mu\text{m}^3 \text{ cm}^{-3}$ during daytime. The volume
10 concentration decreased during the nighttime, although it was still higher than $45.0 \mu\text{m}^3 \text{ cm}^{-3}$.
11 These results demonstrate that the aerosol loading was significantly high during the wildfire haze
12 pollution period.

13 4.2 Chemical characteristics of wildfire haze particles

14 Figures 3a-b show the times series of both mass concentrations and corresponding mass
15 fractions of organics, sulfate, nitrate, ammonium and chloride (expressed as f_{org} , $f_{SO_4^{2-}}$, $f_{NO_3^-}$,
16 $f_{NH_4^+}$, and f_{Cl^-} , respectively, hereinafter) in NR-PM₁ quantified by the ToF-ACSM. The average
17 mass loading of NR-PM₁ was as high as $44.7 \pm 24.5 \mu\text{g m}^{-3}$, confirming the severity of the
18 pervasive wildfire haze. During the observation period, organics was always the most abundant
19 compound in NR-PM₁ ($34.8 \pm 20.7 \mu\text{g m}^{-3}$). The mass concentration of organics was higher than
20 $50.0 \mu\text{g m}^{-3}$ in many cases, and occasionally exceeded $100.0 \mu\text{g m}^{-3}$. On average, organics
21 accounted for the highest mass fraction of 77.1 %, followed by sulfate (11.7 %), ammonium
22 (6.4 %), and nitrate (4.2 %). Mass concentration of chloride was almost negligible (0.6 % of the
23 total mass). These results demonstrate that submicron wildfire haze particles were predominantly
24 composed of organics.

25 Table 2 summarizes the mass concentrations of all the analyzed inorganic ionic species in
26 the PM_{2.5} filter samples. The corresponding data for carbonaceous fractions are presented in
27 Fig. 4. On the whole, the mass fraction of EC varied from 4.4 % to 15.8 % with a mean value of
28 10.8 %. OC occupied 30.4 – 50.7 % of the total PM_{2.5} mass concentration, and the mean fraction
29 is 43.0 %. The WSOC fraction was in the range of 17.6 – 30.2 % with a mean level of 26.7 %.



1 Correspondingly, the water-insoluble OC (WISOC) content was calculated to be 6.1 – 20.5 %
2 with the mean fraction of 16.3 %. The WSOC/OC ratios were constantly higher than 50.0 % with
3 a mean and the maximum values of 63.6 % and 79.9 %, respectively. This result highlights that
4 the majority of organics in the wildfire haze particles were water soluble. Inorganic ions were
5 less abundant and variable than organics. On average, inorganics accounted for 30.5 % of the
6 PM_{2.5} mass loading with the mean contributions of 0.6 % by Cl⁻, 2.6 % by NO₃⁻, 17.2 % by
7 SO₄²⁻, 0.4 % by Na⁺, 8.1 % by NH₄⁺, 0.8 % by K⁺, 0.1 % by Mg²⁺, and 0.7 % by Ca²⁺. Sulfate,
8 ammonium, and nitrate were the most abundant inorganic components. More than half of the
9 inorganics was contributed by sulfate. These results show that wildfire haze particles were
10 dominated by organics, especially water-soluble species. Mass concentrations of organics
11 measured by PM_{2.5} filter samples and by the ToF-ACSM agreed well when organics/OC ratio
12 was assumed as 1.4 (slope = 1.07; $R^2 = 0.91$) (Reid et al., 2005; Hallquist et al., 2009; Levin et
13 al., 2010). The total mass concentrations of aerosol particles quantified by the filter samples and
14 the ToF-ACSM also correlated well ($R^2 = 0.96$). The mass loading of the PM_{2.5} filter samples
15 was approximately 30 % higher than that of the ToF-ACSM results, likely because of the
16 difference in particle size range and lack of EC content for the ToF-ACSM measurements
17 (Budisulistiorini et al., in preparation).

18 Figure 3c shows the mean mass spectra of organics averaged over the observation period.
19 Ion signals at m/z 43 (most likely C₂H₃O⁺) and m/z 44 (CO₂⁺) were prominent, accounting for
20 7.5 % and 10.5 % of the total organics mass spectrum. The predominant signal of m/z 44
21 indicates that organic compounds in wildfire haze particles were highly oxygenated. High-
22 molecular weight organic constituents with $m/z > 100$ possess an abundance of 13.3 % in total.
23 Marker ions for biomass burning particles such as m/z 60 (mostly C₂H₄O₂⁺) and m/z 73 (mainly
24 C₃H₅O₂⁺), those originating from levoglucosan-like species (e.g., levoglucosan, mannosan, and
25 galactosan) were also clearly observed (Cubison et al., 2011).

26 Figure 6d shows mean contributions of four organic components classified by the ME-2
27 method, including HOA (8.8 % of NR-PM₁ mass), PBOA (10.4 %), BBOA (10.0 %), and OOA
28 (36.0 %). Primary organics originating from biomass burning (i.e., PBOA and BBOA) accounted
29 for 20.4 % in total. OOA was the dominant type of organics during wildfire haze episodes.



1 **4.3 Hygroscopic properties of wildfire haze particles**

2 Figure 5 displays the time series of mean GF data as well as corresponding values of κ
3 during the whole observation period. The mean values of GF varied between 0.98 and 1.52 with
4 the average of 1.25 ± 0.09 . GF values larger than 1.40 were normally observed after noontime.
5 The variation of corresponding κ results spanned from 0.004 – 0.475, and the average of κ value
6 was 0.189 ± 0.087 . Table 3 summarizes the mean κ results of organics (cf. Sect.3.2, with EC
7 considered) calculated from the HTDMA and ToF-ACSM measurements during the overlapping
8 observation period of 10 – 24 October 2015. The HTDMA-derived bulk κ results averaged over
9 the same overlapping period is defined as κ_{HTDMA} . The mean κ_{org} (0.157 ± 0.108) is lower than
10 the mean κ_{OOA} (0.287 ± 0.193), as the whole organic fraction normally contains both non-
11 hygroscopic and hygroscopic organics. The derived κ_{org} and κ_{OOA} results are demonstrated to be
12 fairly comparable to previously reported κ values for bulk organics and highly oxygenated water-
13 soluble organic fraction, respectively (Petters and Kreidenweis, 2007; Chang et al., 2010;
14 Duplissy et al., 2011; Lathem et al., 2013; Cerully et al., 2015; Ogawa et al., 2016; Chen et al.,
15 2017). Note that the mean κ_{OOA} is even higher than the corresponding mean κ_{HTDMA} ($0.207 \pm$
16 0.093), revealing that the water uptake by the organic fraction particularly some highly
17 oxygenated organics in the wildfire haze particles could be quite significant.

18 **4.4 Diurnal variations of hygroscopic properties and chemical composition**

19 GF exhibits a clear pattern of diurnal variation (Fig. 6a). Higher GF values were
20 observed during the daytime ($GF = 1.27 \pm 0.05$ for 08:00 – 20:00 LT). On the other hand, the
21 value was lower in the early morning and nighttime (1.23 ± 0.05 for 20:00 – 08:00 LT). The
22 corresponding mean bulk κ results averaged over the whole observation period were $0.213 \pm$
23 0.051 for the daytime and 0.172 ± 0.043 for nighttime.

24 Similarly, the daytime mean κ_{org} and κ_{OOA} are 0.200 ± 0.104 and 0.353 ± 0.179 ,
25 respectively, whereas the nighttime mean values are 0.103 ± 0.086 (κ_{org}) and 0.206 ± 0.178 (κ_{OOA})
26 (Table 3). These mean κ values are 19.2 % lower (κ_{org}) and 42.8 % higher (κ_{OOA}) than the
27 concurrently measured mean κ_{HTDMA} result of 0.247 ± 0.096 (daytime), whilst 35.9 % lower (κ_{org})
28 and 28.2 % higher (κ_{OOA}) than that of 0.160 ± 0.063 (nighttime). A more significant discrepancy
29 between κ_{org} and κ_{HTDMA} is observed for the nighttime case (whereas a larger difference between



1 κ_{org} and κ_{HTDMA} occurs during daytime), likely due to the greatly inhibited organics oxidation
2 processes in the evening compared to the enhanced situation during daytime. Such a correlation
3 could somewhat be visually clued from the corresponding diurnal patterns of both mean GF and
4 OA factors, as the fraction of OOA is demonstrated as a moderately good indicator of the
5 hygroscopicity of organics (Ogawa et al., 2016).

6 The observed variation of GF was dominantly caused by diurnal variation in probability
7 distribution of g (Fig. 6b). Namely, number fractions of highly hygroscopic mode particles were
8 low in the early morning and evening ($nf_{highly} < 0.3$), and higher during afternoon (approaching
9 the highest level of 0.6 around 15:00 LT). The value positively correlated with GF ($R = 0.97$).
10 The number fraction of weakly hygroscopic mode particles was opposite of that for highly
11 hygroscopic particles, and negatively correlated with mean GF ($R = -0.95$). There was no clear
12 diurnal variation for the number fraction of moderately hygroscopic mode particles (stable
13 around 0.2). These results suggest that water uptake by wildfire haze particles are tightly related
14 to the fractions of weakly and highly hygroscopic mode particles. The mean g values for each
15 mode were 1.05 ± 0.02 for weakly, 1.21 ± 0.01 for moderately, and 1.40 ± 0.05 for highly
16 hygroscopic particles. The average values for nf were 0.42 ± 0.18 for weakly, 0.18 ± 0.07 for
17 moderately, and 0.40 ± 0.20 for highly hygroscopic particles (Table 4).

18 The diurnal variation in hygroscopic properties coincides with that in chemical
19 composition (Fig. 6c). The mean GF correlated well with $f_{SO_4^{2-}}$, suggesting the primary role of
20 $f_{SO_4^{2-}}$ in governing the water uptake by wildfire haze particles. The enhancement of $f_{SO_4^{2-}}$
21 accompanied decrease of f_{org} . Variation of chemical composition of organics also correlated well
22 with water uptake properties. The fractional of signal intensity at m/z 44 (f_{44}), which is
23 considered as a marker ion for degree of oxidation (Duplissy et al., 2011; Ng et al., 2011; Ogawa
24 et al., 2016), was also high during daytime, as in the case of mean GF and $f_{SO_4^{2-}}$. A similar
25 pattern was also observed for f_{OOA} , while that for HOA was opposite. For instance, f_{HOA} was the
26 highest during morning rush hours, and subsequently decreased during daytime. Variation of the
27 fresh PBOA fraction (f_{PBOA}) is kind of similar to that of non-peat BBOA (f_{BBOA}), i.e., without an
28 apparent diurnal pattern during the severe wildfire haze periods.



1 The diurnal variation in change of organic composition was caused by enhanced f_{OOA}
2 during daytime, which accompanied decrease in f_{HOA} . In general, highly oxygenated organic
3 compounds are highly hygroscopic due to their water solubility, qualitatively explaining the
4 similarity in diurnal variations among mean GF , f_{OOA} , and f_{44} (Duplissy et al., 2011; Zhao et al.,
5 2015; Ogawa et al., 2016). The relationship between particle hygroscopicity and degree of
6 oxidation of organics will be discussed in detail in Sect.5.2.

7

8 **5. Discussions**

9 **5.1 Chemical composition dependences of water uptake by wildfire haze particles**

10 Figure 7 depicts the relationships between κ and mass fractions of both inorganic species
11 and organics in NR-PM₁ both for daytime and nighttime data. κ and $f_{SO_4^{2-}}$ positively correlate,
12 demonstrating that sulfate is the most important compound in governing water uptake by 100 nm
13 wildfire haze particles due to its high hygroscopicity. Similarly, κ is positively related to $f_{NH_4^+}$, as
14 it is the counter anion of sulfate. On the contrary, κ negatively correlates with f_{org} , as organics are
15 less hygroscopic than inorganic salts. There is no clear correlation between κ and $f_{NO_3^-}$, implying
16 that nitrate is not the major contributor to the variability of κ . κ is almost independent of f_{Cl^-} ,
17 partially due to the limited availability of chloride.

18 The correlation between κ and f_{org} is relatively scattered. For instance, κ can vary from
19 0.10 to 0.40 when f_{org} is 0.7, meaning that some other factors than f_{org} may also influence water
20 uptake. Variability in chemical characteristics of organics might have played a role in the scatter
21 of the data (Fig. 6d and e).

22 **5.2 Relationship between hygroscopicity and chemical composition of organics**

23 Table 2 summarizes the κ_{org} and κ_{OOA} results averaged over the same PM_{2.5} filter
24 sampling periods. Figure 8 illustrates the relationship between κ_{org} and f_{WSOC} . In general, κ_{org}
25 loosely correlates with f_{WSOC} to some extent, except for the data on October 22nd. The relatively
26 high value of f_{44} (0.11) on October 22nd might be the cause of the deviation. These results



1 indicate the importance of both the WSOC fraction and oxygenation degree of organics in the
2 hygroscopic growth.

3 Figure 9 depicts the relationships between κ_{org} and f_{44} as well as κ_{org} and f_{44}/f_{43} . Daily
4 average data were utilized. Although the data are scattered, a positive correlation between κ_{org}
5 and f_{44} was observed ($R = 0.70$). The signal of m/z 44 (mostly CO_2^+) is known to originate from
6 highly oxidized organic functional groups such as dicarboxylic acids and acyl peroxides (Aiken
7 et al., 2008). These highly oxygenated functional groups contribute in promoting hygroscopicity
8 by enhancing water solubility (Topping et al., 2005; Cubison et al., 2006; Hallquist et al., 2009;
9 Duplissy et al., 2011; Psichoudaki and Pandis, 2013; Suda et al., 2014; Riipinen et al., 2015;
10 Ogawa et al., 2016; Petters et al., 2016; Marsh et al., 2017). κ_{org} and f_{44}/f_{43} also presented a
11 similar trend to that of κ_{org} and f_{44} . The correlations shown in Fig. 9 clearly demonstrate the
12 important role of oxygenation degree in water uptake properties of organic compounds in
13 wildfire haze particles.

14 During daytime, organic particles tend to be highly oxidized due to oxidation of primary
15 organic aerosol as well as formation of secondary organic aerosol from volatile organic
16 compounds (Fig. 6, Ng et al., 2010; Zhao et al., 2016). These chemical evolution processes of
17 organic aerosol particles will need to be better understood for quantitative prediction of water
18 uptake by wildfire haze particles (Kroll and Seinfeld, 2008; Riipinen et al., 2011; Winkler et al.,
19 2012; Ehn et al., 2014). The evolution process could induce alternation in size-dependence in
20 chemical composition as well as in mixing state (Chakrabarty et al., 2006; Zhao et al., 2015). To
21 unveil these unanswered questions, more details of the size- and mixing state dependent
22 chemical compositions as well as molecular level chemical characteristics of Indonesian wildfire
23 haze particles will be required.

24

25 6. Conclusions

26 In September – October 2015, Indonesian wildfire-induced transboundary haze pollution
27 spread through Southeast Asia, affecting both environment and climate dramatically and
28 ravaging public health and the economy seriously. As a downwind receptor city, Singapore



1 experienced the pervasive wildfire haze events. During the periods, we simultaneously measured
2 hygroscopic growth factors (*GF*) and chemical compositions of ambient wildfire haze particles
3 in Singapore, targeting for more comprehensive insights into the linkages between water uptake
4 and particle chemical composition as well as secondary aerosol formation.

5 High aerosol loading of non-refractory submicron particles (NR-PM₁, occasionally
6 exceeding 100.0 μg m⁻³) was frequently observed, stressing the severity of the 2015 wildfire
7 haze pollution. The NR-PM₁ particles are predominantly composed of organics (OA,
8 approximately 77.1 % on average) and sulfate dominates the inorganic constituents (about
9 11.7 %). Chemical analyses of NR-PM₁ indicate the ubiquity and dominance of oxygenated
10 species in organics, in line with the most intense ion signals at *m/z* 44 (mostly CO₂⁺, *f*₄₄ = 10.5 %
11 in total OA mass) and *m/z* 43 (most likely C₂H₃O⁺, *f*₄₃ = 7.5 % on average). Moreover, a major
12 fraction of organics is water soluble, as signified by the high water-soluble organic carbon
13 fraction in ambient PM_{2.5} filter samples (26.7 % of the total PM_{2.5} mass).

14 Wildfire haze particles are generally highly hygroscopic. The hygroscopicity parameter, κ ,
15 of 100 nm particles varies between 0.004 and 0.475, with a mean κ value of 0.189 ± 0.087 . The
16 derived mean κ results of organics are 0.157 ± 0.108 (κ_{org} , bulk organics) and 0.287 ± 0.193
17 (κ_{OOA} , oxygenated organic fraction), fairly comparable to the reported values for organic
18 compounds (Petters and Kreidenweis, 2007; Duplissy et al., 2011; Latham et al., 2013; Cerully et
19 al., 2015). This highlights the difference in κ between wildfire haze particles and fresh
20 Indonesian peat burning particles, which are intrinsically non-hygroscopic due to the rather
21 limited water-soluble organic fraction (Chen et al., 2017). *GF* data show a notable diurnal
22 variation that commonly peaks during the daytime. This is identical with the diurnal pattern of
23 number fraction of highly hygroscopic mode particles and accompanied opposite fluctuation of
24 number fraction of weakly hygroscopic mode. These results imply the chemical composition
25 dependence of particle hygroscopicity, verified by the fact that κ is positively correlated with
26 mass fraction of sulfate but inversely related to the mass fraction of organics. Aside from the
27 governing influence of sulfate, κ of haze particles is also contributed by water uptake of organics.
28 κ_{org} is loosely related to the water-soluble organic fraction, yet a positive correlation between κ_{org}
29 and *f*₄₄ was shown ($R = 0.70$). This denotes that the oxygenation degree of organics may play an
30 important role in water uptake especially by organic-rich haze particles.



1 To our knowledge, this could be the first reported field water uptake measurements of
2 wildfire haze particles in Equatorial Asia. The presented results suggest that formation of
3 secondary aerosol particles, including both inorganics and organics, is the key in addressing the
4 variability in reported data on hygroscopic properties of aerosol particles originating from
5 Indonesian peatland fires. Size-dependent chemical composition as well as further detailed
6 chemical analysis will be needed in future studies for quantitative understanding on water uptake
7 by Indonesian wildfire-induced particles.

8

9 **Acknowledgements**

10 This work was supported by the Singapore National Research Foundation (NRF) under
11 its Singapore National Research Fellowship scheme (National Research Fellow Award,
12 NRF2012NRF-NRFF001-031), NRF Campus for Research Excellence and Technological
13 Enterprise (CREATE) program (NRF2016-ITCOO1-021), the Earth Observatory of Singapore,
14 and Nanyang Technological University. Takuma Miyakawa and Yuichi Komazaki were funded
15 by the Environment Research and Technology Development Fund (2-1403) of the Ministry of
16 Environment, Japan, and the Japan Society for the Promotion of Science (JSPS),
17 KAKENHI Grant number JP26550021. We would like to thank Wen-Chien Lee and Gissella B.
18 Lebron for assisting in the ambient haze observations. We also acknowledge the help of Pavel
19 Adamek in polishing our English.



1 **References:**

- 2 Aiken, A. C., DeCarlo, P. F., Kroll, J. H., Worsnop, D. R., Huffman, J. A., Docherty, K. S.,
3 Ulbrich, I. M., Mohr, C., Kimmel, J. R., Sueper, D., Sun, Y., Zhang, Q., Trimborn, A., Northway,
4 M., Ziemann, P. J., Canagaratna, M. R., Onasch, T. B., Alfarra, M. R., Prevot, A. S. H., Dommen,
5 J., Duplissy, J., Metzger, A., Baltensperger, U., and Jimenez, J. L. (2008). O/C and OM/OC
6 ratios of primary, secondary, and ambient organic aerosols with high-resolution time-of-flight
7 aerosol mass spectrometry, *Environ. Sci. Technol.*, 42, 4478-4485.
- 8 Allan, J. D., Jimenez, J. L., Williams, P. I., Alfarra, M. R., Bower, K. N., Jayne, J. T., Coe, H.,
9 Worsnop, D. R. (2003). Quantitative sampling using an Aerodyne aerosol mass spectrometer 1.
10 Techniques of data interpretation and error analysis. *J. Geophys. Res. Atmos.*, 108, 4090.
- 11 Balasubramanian, R., Qian, W.-B., Decesari, S., Facchini, M. C., Fuzzi, S. (2003).
12 Comprehensive characterization of PM_{2.5} aerosols in Singapore. *J. Geophys. Res. Atmos.*, 108,
13 4523.
- 14 Bond, T. C., and Bergstrom, R. W. (2006). Light absorption by carbonaceous particles: An
15 investigative review. *Aerosol Sci. & Technol.*, 40, 27-67.
- 16 Bougiatioti, A., Bezantakos, S., Stavroulas, I., Kalivitis, N., Kokkalis, P., Biskos, G.,
17 Mihalopoulos, N., Papayannis, A., and Nenes, A. (2016). Biomass-burning impact on CCN
18 number, hygroscopicity and cloud formation during summertime in the eastern Mediterranean.
19 *Atmos. Chem. Phys.*, 16, 7389-7409.
- 20 Brechtel, F. J., and Kreidenweis, S. M. (2000). Predicting particle critical supersaturation from
21 hygroscopic growth measurements in the humidified TDMA. Part II: laboratory and ambient
22 studies. *J. Atmos. Sci.*, 57, 1872-1887.
- 23 Canonaco, F., Crippa, M., Slowik, J. G., Baltensperger, U., and Prévôt, A. S. H. (2013). SoFi, an
24 IGOR-based interface for the efficient use of the generalized multilinear engine (ME-2) for the
25 source apportionment: ME-2 application to aerosol mass spectrometer data. *Atmos. Meas. Tech.*,
26 6, 3649-3661.
- 27 Carrico, C. M., Petters, M. D., Kreidenweis, S. M., Collett Jr., J. L., Engling, G., Malm, W. C.
28 (2008). Aerosol hygroscopicity and cloud droplet activation of extracts of filters from biomass
29 burning experiments. *J. Geophys. Res. Atmos.*, 113, D08206.
- 30 Carrico, C. M., Petters, M. D., Kreidenweis, S. M., Sullivan, A. P., McMeeking, G. R., Levin, E.
31 J. T., Engling, G., Malm, W. C., and Collett Jr., J. L. (2010). Water uptake and chemical
32 composition of fresh aerosols generated in open burning of biomass. *Atmos. Chem. Phys.*, 10,
33 5165-5178.
- 34 Cerully, K. M., Bougiatioti, A., Hite Jr, J. R., Guo, H., Xu, L., Ng, N. L., Weber, R., Nenes, A.
35 (2015). On the link between hygroscopicity, volatility, and oxidation state of ambient and water-
36 soluble aerosols in the southeastern United States. *Atmos. Chem. Phys.*, 15, 8679-8694.
- 37 Chakrabarty, R. K., Moosmuller, H., Garro, M. A., Arnott, W. P., Walker, J., Susott, R. A.,
38 Babbitt, R. E., Wold, C. E., Lincoln, E. N., and Hao, W. M. (2006). Emissions from the
39 laboratory combustion of wildland fuels: Particle morphology and size, *J. Geophys. Res.*, 111,
40 D07204.



- 1 Chan, M. N., and Chan, C. K. (2003). Hygroscopic properties of two model humic-like
2 substances and their mixtures with inorganics of atmospheric importance. *Environ. Sci. &*
3 *Technol.*, 37, 5109-5115.
- 4 Chan, M. N., Choi, M. Y., Ng, N. L., Chan, C. K. (2005). Hygroscopicity of water-soluble
5 organic compounds in atmospheric aerosols: Amino acids and biomass burning derived organic
6 species. *Environ. Sci. & Technol.*, 39, 1555-1562.
- 7 Chand, D., Schmid, O., Gwaze, P., Parmar, R. S., Helas, G., Zeromskiene, K., Wiedensohler, A.,
8 Massling, A., Andreae, M. O. (2005). Laboratory measurements of smoke optical properties
9 from the burning of Indonesian peat and other types of biomass. *Geophys. Res. Lett.*, 32, L12819.
- 10 Chang, R. Y. W., Slowik, J. G., Shantz, N. C., Vlasenko, A., Liggio, J., Sjostedt, S. J., Leitch,
11 W. R., and Abbatt, J. P. D. (2010). The hygroscopicity parameter (κ) of ambient organic aerosol
12 at a field site subject to biogenic and anthropogenic influences: relationship to degree of aerosol
13 oxidation. *Atmos. Chem. Phys.*, 10, 5047-5064.
- 14 Chen, J., Budisulistiorini, S. H., Itoh, M., Lee, W.-C., Miyakawa, T., Komazaki, Y., Yang, L.,
15 Kuwata, M. (2017). Water uptake by fresh Indonesian peat burning particles is limited by water
16 soluble organic matter. *Atmos. Chem. Phys.*, 17, 11591-11604.
- 17 Chow, J. C., Watson, J. G., Pritchett, L. C., Pierson, W. R., Frazier, C. A., and Purcell, R. G.
18 (1993): The DRI thermal/optical reflectance carbon analysis system: Description, evaluation and
19 applications in U.S. air quality studies, *Atmos. Environ.*, 27A, 1185-1201.
- 20 Crippa, P., Castruccio, S., Archer-Nicholls, S., Lebron, G. B., Kuwata, M., Thota, A., Sumin, S.,
21 Butt, E., Wiedinmyer, C., Spracklen, D. V. (2016). Population exposure to hazardous air quality
22 due to the 2015 fires in Equatorial Asia. *Sci. Rep.*, 6, 37074.
- 23 Cross, E. S., Slowik, J. G., Davidovits, P., Allan, J. D., Worsnop, D. R., Jayne, J. T., Lewis, D.
24 K., Canagaratna, M., and Onasch, T. B. (2007). Laboratory and ambient particle density
25 determinations using light scattering in conjunction with aerosol mass spectrometry. *Aerosol Sci.*
26 *Technol.*, 41, 343-359.
- 27 Cubison, M. J., Alfarra, M. R., Allan, J., Bower, K. N., Coe, H., McFiggans, G. B., Whitehead, J.
28 D., Williams, P. I., Zhang, Q., Jimenez, J. L., Hopkins, J., and Lee, J. (2006). The
29 characterisation of pollution aerosol in a changing photochemical environment. *Atmos. Chem.*
30 *Phys.*, 6, 5573-5588.
- 31 Cubison, M. J., Ortega, A. M., Hayes, P. L., Farmer, D. K., Day, D., Lechner, M. J., Brune, W.
32 H., Apel, E., Diskin, G. S., Fisher, J. A., Fuelberg, H. E., Hecobian, A., Knapp, D. J., Mikoviny,
33 T., Riemer, D., Sachse, G. W., Sessions, W., Weber, R. J., Weinheimer, A. J., Wisthaler, A.,
34 Jimenez, J. L. (2011). Effects of aging on organic aerosol from open biomass burning smoke in
35 aircraft and laboratory studies. *Atmos. Chem. Phys.*, 11, 12049-12064.
- 36 Dick, W. D., Saxena, P., and McMurry, P. H. (2000). Estimation of water uptake by organic
37 compounds in submicron aerosols measured during the Southeastern Aerosol and Visibility
38 Study. *J. Geophys. Res. Atmos.*, 105, 1471-1479.
- 39 Dinar, E., Taraniuk, I., Graber, E. R., Anttila, T., Mentel, T. F., and Rudich, Y. (2007).
40 Hygroscopic growth of atmospheric and model humic-like substances, *J. Geophys. Res.*, 112,
41 D05211.



- 1 Duncan, B. N., Bey, I., Chin, M., Mickley, L. J., Fairlie, T. D., Martin, R. V., Matsueda, H.
2 (2003). Indonesian wildfires of 1997: Impact on tropospheric chemistry. *J. Geophys. Res.*
3 *Atmos.*, 108, 4458.
- 4 Duplissy, J., DeCarlo, P. F., Dommen, J., Alfarra, M. R., Metzger, A., Barmapadimos, I., Prevot,
5 A. S. H., Weingartner, E., Tritscher, T., Gysel, M., Aiken, A. C., Jimenez, J. L., Canagaratna, M.
6 R., Worsnop, D. R., Collins, D. R., Tomlinson, J., and Baltensperger, U. (2011). Relating
7 hygroscopicity and composition of organic aerosol particulate matter. *Atmos. Chem. Phys.*, 11,
8 1155-1165.
- 9 Duplissy, J., Gysel, M., Alfarra, M. R., Dommen, J., Metzger, A., Prévôt, A. S. H., Weingartner,
10 E., Laaksonen, A., Raatikainen, T., Good, N., Turner, S. F., McFiggans, G., and Baltensperger,
11 U. (2008). Cloud forming potential of secondary organic aerosol under near atmospheric
12 conditions, *Geophys. Res. Lett.*, 35, L03818.
- 13 Duplissy, J., Gysel, M., Sjogren, S., Meyer, N., Good, N., Kammermann, L., Michaud, V.,
14 Weigel, R., Martins dos Santos, S., Gruening, C., Villani, P., Laj, P., Sellegri, K., Metzger, A.,
15 McFiggans, G. B., Wehrle, G., Richter, R., Dommen, J., Ristovski, Z., Baltensperger, U.,
16 Weingartner, E. (2009). Intercomparison study of six HTDMAs: results and recommendations.
17 *Atmos. Meas. Tech.*, 2, 363-378.
- 18 Dusek, U., Frank, G. P., Helas, G., Iinuma, Y., Zeromskiene, K., Gwaze, P., Hennig, T.,
19 Massling, A., Schmid, O., Herrmann, H., Wiedensohler, A., Andreae, M. O. (2005). “Missing”
20 cloud condensation nuclei in peat smoke. *Geophys. Res. Lett.*, 32, L11802.
- 21 Ehn, M., Thornton, J. A., Kleist, E., Sipila, M., Junninen, H., Pullinen, I., Springer, M., Rubach,
22 F., Tillmann, R., Lee, B., Lopez-Hilfiker, F., Andres, S., Acir, I.-H., Rissanen, M., Jokinen, T.,
23 Schobesberger, S., Kangasluoma, J., Kontkanen, J., Nieminen, T., Kurten, T., Nielsen, L. B.,
24 Jorgensen, S., Kjaergaard, H. G., Canagaratna, M., Maso, M. D., Berndt, T., Petaja, T., Wahner,
25 A., Kerminen, V.-M., Kulmala, M., Worsnop, D. R., Wildt, J., and Mentel, T. F. (2014). A large
26 source of low-volatility secondary organic aerosol. *Nature*, 506, 476-479.
- 27 Field, R. D., van der Werf, G. R., Fanin, T., Fetzer, E. J., Fuller, R., Jethva, H., Levy, R., Livesey,
28 N. J., Luo, M., Torres, O., and Worden, H. M. (2016). Indonesian fire activity and smoke
29 pollution in 2015 show persistent nonlinear sensitivity to El Niño-induced drought. *Proc. Natl.*
30 *Acad. Sci.*, 113, 9204-9209.
- 31 Fröhlich, R., Cubison, M. J., Slowik, J. G., Bukowiecki, N., Prévôt, A. S. H., Baltensperger, U.,
32 Schneider, J., Kimmel, J. R., Gonin, M., Rohner, U., Worsnop, D. R., Jayne, J. T. (2013). The
33 ToF-ACSM: a portable aerosol chemical speciation monitor with TOFMS detection. *Atmos.*
34 *Meas. Tech.*, 6, 3225-3241.
- 35 Gras, J. L., Jensen, J. B., Okada, K., Ikegami, M., Zaizen, Y., Makino, Y. (1999). Some optical
36 properties of smoke aerosol in Indonesia and tropical Australia. *Geophys. Res. Lett.*, 26, 1393-
37 1396.
- 38 Gunthe, S. S., King, S. M., Rose, D., Chen, Q., Roldin, P., Farmer, D. K., Jimenez, J. L., Artaxo,
39 P., Andreae, M. O., Martin, S. T., and Pöschl, U. (2009). Cloud condensation nuclei in pristine
40 tropical rainforest air of Amazonia: size-resolved measurements and modeling of atmospheric
41 aerosol composition and CCN activity. *Atmos. Chem. Phys.*, 9, 7551-7575.



- 1 Gysel, M., Crosier, J., Topping, D. O., Whitehead, J. D., Bower, K. N., Cubison, M. J., Williams,
2 P. I., Flynn, M. J., McFiggans, G. B., Coe, H. (2007). Closure study between chemical
3 composition and hygroscopic growth of aerosol particles during TORCH2. *Atmos. Chem. Phys.*,
4 7, 6131-6144.
- 5 Gysel, M., McFiggans, G. B., Coe, H. (2009). Inversion of tandem differential mobility analyser
6 (TDMA) measurements. *J. Aerosol Sci.*, 40, 134-151.
- 7 Gysel, M., Weingartner, E., Nyeki, S., Paulsen, D., Baltensperger, U., Galambos, I., Kiss, G.
8 (2004). Hygroscopic properties of water-soluble matter and humic-like organics in atmospheric
9 fine aerosol. *Atmos. Chem. Phys.*, 4, 35-50.
- 10 Hallar, A. G., Lowenthal, D. H., Clegg, S. L., Samburova, V., Taylor, N., Mazzoleni, L. R.,
11 Zielinska, B. K., Kristensen, T. B., Chirokova, G., McCubbin, I. B., Dodson, C., and Collins, D.
12 (2013). Chemical and hygroscopic properties of aerosol organics at Storm Peak Laboratory. *J.*
13 *Geophys. Res. Atmos.*, 118, 4767-4779.
- 14 Hallquist, M., Wenger, J. C., Baltensperger, U., Rudich, Y., Simpson, D., Claeys, M., Dommen,
15 J., Donahue, N. M., George, C., Goldstein, A. H., Hamilton, J. F., Herrmann, H., Hoffmann, T.,
16 Iinuma, Y., Jang, M., Jenkin, M. E., Jimenez, J. L., Kiendler-Scharr, A., Maenhaut, W.,
17 McFiggans, G., Mentel, Th. F., Monod, A., Prévôt, A. S. H., Seinfeld, J. H., Surratt, J. D.,
18 Szmigielski, R., and Wildt, J. (2009). The formation, properties and impact of secondary organic
19 aerosol: current and emerging issues, *Atmos. Chem. Phys.*, 9, 5155-5236.
- 20 Huijnen, V., Wooster, M. J., Kaiser, J. W., Gaveau, D. L. A., Flemming, J., Parrington, M.,
21 Inness, A., Murdiyarto, D., Main, B., and van Weele, M. (2016). Fire carbon emissions over
22 maritime southeast Asia in 2015 largest since 1997, *Sci. Rep.*, 6, 26886.
- 23 Jimenez, J. L., Canagaratna, M. R., Donahue, N. M., Prevot, A. S. H., Zhang, Q., Kroll, J. H.,
24 DeCarlo, P. F., Allan, J. D., Coe, H., Ng, N. L., Aiken, A. C., Docherty, K. S., Ulbrich, I. M.,
25 Grieshop, A. P., Robinson, A. L., Duplissy, J., Smith, J. D., Wilson, K. R., Lanz, V. A., Hueglin,
26 C., Sun, Y. L., Tian, J., Laaksonen, A., Raatikainen, T., Rautiainen, J., Vaattovaara, P., Ehn, M.,
27 Kulmala, M., Tomlinson, J. M., Collins, D. R., Cubison, M. J., Dunlea, J., Huffman, J. A.,
28 Onasch, T. B., Alfarra, M. R., Williams, P. I., Bower, K., Kondo, Y., Schneider, J., Drewnick, F.,
29 Borrmann, S., Weimer, S., Demerjian, K., Salcedo, D., Cottrell, L., Griffin, R., Takami, A.,
30 Miyoshi, T., Hatakeyama, S., Shimono, A., Sun, J. Y., Zhang, Y. M., Dzepina, K., Kimmel, J. R.,
31 Sueper, D., Jayne, J. T., Herndon, S. C., Trimborn, A. M., Williams, L. R., Wood, E. C.,
32 Middlebrook, A. M., Kolb, C. E., Baltensperger, U., Worsnop, D. R. (2009). Evolution of
33 organic aerosols in the atmosphere. *Science*, 326, 1525-1529.
- 34 Johnston, F. H., Henderson, S.B., Chen, Y., Randerson, J. T., Marlier, M., DeFries, R. S., Kinney,
35 P., Bowman, D. M., Brauer, M. (2012). Estimated global mortality attributable to smoke from
36 landscape fires. *Environ. Health Perspect.*, 120, 695-701.
- 37 Keywood, M. D., Ayers, G. P., Gras, J. L., Boers, R., Leong, C. P. (2003). Haze in the Klang
38 Valley of Malaysia. *Atmos. Chem. Phys.*, 3, 591-605.
- 39 King, S. M., Rosenoern, T., Shilling, J. E., Chen, Q., and Martin, S. T. (2007). Cloud
40 condensation nucleus activity of secondary organic aerosol particles mixed with sulfate, *Geophys.*
41 *Res. Lett.*, 34, L24803.



- 1 Konecny, K., Ballhorn, U., Navratil, P., Jubanski, J., Page, S. E., Tansey, K., Hooijer, A.,
2 Vernimmen, R., and Siegert, F. (2016). Variable carbon losses from recurrent fires in drained
3 tropical peatlands. *Glob. Change Biol.*, 22, 1469-1480.
- 4 Koplitz, S. N., Mickley, L. J., Marlier, M. E., Buonocore, J. J., Kim, P. S., Liu, T., Sulprizio, M.
5 P., DeFries, R. S., Jacob, D. J., Schwartz, J., Pongsiri, M., and Myers, S. S. (2016). Public health
6 impacts of the severe haze in Equatorial Asia in September–October 2015: demonstration of a
7 new framework for informing fire management strategies to reduce downwind smoke exposure.
8 *Environ. Res. Lett.*, 11, 094023.
- 9 Kreidenweis, S. M., Petters, M. D., and DeMott, P. J. (2008). Single-parameter estimates of
10 aerosol water content, *Environ. Res. Lett.*, 3, 035002.
- 11 Kristensen, T. B., Wex, H., Nekat, B., Nøjgaard, J. K., van Pinxteren, D., Lowenthal, D. H.,
12 Mazzoleni, L. R., Dieckmann, K., Bender Koch, C., Mentel, T. F., Herrmann, H., Hallar, A. G.,
13 Stratmann, F., and Bilde, M. (2012). Hygroscopic growth and CCN activity of HULIS from
14 different environments. *J. Geophys. Res. Atmos.*, 117, D22203.
- 15 Kroll, J. H., and Seinfeld, J. H. (2008). Chemistry of secondary organic aerosol: Formation and
16 evolution of low-volatility organics in the atmosphere, *Atmos. Environ.*, 42, 3593-3624.
- 17 Kunii, O., Kanagawa, S., Yajima, I., Hisamatsu, Y., Yamamura, S., Amagai, T., Ismail, Ir T. S.
18 (2002). The 1997 haze disaster in Indonesia: Its air quality and health effects. *Archives of*
19 *Environmental Health: An International Journal*, 57, 16-22.
- 20 Kuwata, M., Zorn, S. R., and Martin, S. T. (2012). Using elemental ratios to predict the density
21 of organic material composed of carbon, hydrogen, and oxygen. *Environ. Sci. & Technol.*, 46,
22 787-794.
- 23 Langner A, Miettinen J, and Siegert F. (2007). Land cover change 2002–2005 in Borneo and the
24 role of fire derived from MODIS imagery. *Glob. Change Biol.*, 13, 2329-2340.
- 25 Lanz, V. A., Alfarra, M. R., Baltensperger, U., Buchmann, B., Hueglin, C., Prévôt, A. S. H.
26 (2007). Source apportionment of submicron organic aerosols at an urban site by factor analytical
27 modelling of aerosol mass spectra. *Atmos. Chem. Phys.*, 7, 1503-1522.
- 28 Latham, T. L., Beyersdorf, A. J., Thornhill, K. L., Winstead, E. L., Cubison, M. J., Hecobian, A.,
29 Jimenez, J. L., Weber, R. J., Anderson, B. E., Nenes, A. (2013). Analysis of CCN activity of
30 Arctic aerosol and Canadian biomass burning during summer 2008. *Atmos. Chem. Phys.*, 13,
31 2735-2756.
- 32 Lelieveld, J., Evans, J. S., Fnais, M., Giannadaki, D., and Pozzer, A. (2015). The contribution of
33 outdoor air pollution sources to premature mortality on a global scale. *Nature*, 525, 367-371.
- 34 Levin, E. J. T., McMeeking, G. R., Carrico, C. M., Mack, L., Kreidenweis, S. M., Wold, C. E.,
35 Moosmueller, H., Arnott, W. P., Hao, W. M., Collett, J. L., and Malm, W. C. (2010). Biomass
36 burning smoke aerosol properties measured during FLAME 2, *J. Geophys. Res.*, 115, D18210.
- 37 Lin, N.-H., Tsay, S.-C., Maring, H. B., Yen, M.-C., Sheu, G.-R., Wang, S.-H., Chi, K. H.,
38 Chuang, M.-T., Ou-Yang, C.-F., Fu, J. S., Reid, J. S., Lee, C.-T., Wang, L.-C., Wang, J.-L., Hsu,
39 C. N., Sayer, A. M., Holben, B. N., Chu, Y.-C., Nguyen, X. A., Sopajaree, K., Chen, S.-J.,
40 Cheng, M.-T., Tsuang, B.-J., Tsai, C.-J., Peng, C.-M., Schnell, R. C., Conway, T., Chang, C.-T.,
41 Lin, K.-S., Tsai, Y. I., Lee, W.-J., Chang, S.-C., Liu, J.-J., Chiang, W.-L., Huang, S.-J., Lin, T.-



- 1 H., and Liu, G.-R. (2013). An overview of regional experiments on biomass burning aerosols and
2 related pollutants in Southeast Asia: From BASE-ASIA and the Dongsha Experiment to 7-SEAS.
3 Atmos. Environ., 78, 1-19.
- 4 Marcolli C., Luo B., and Peter, T. (2004). Mixing of the organic aerosol fractions: liquids as the
5 thermodynamically stable phases. J. Phys. Chem. A, 108, 2216-2224.
- 6 Marlier, M. E., DeFries, R. S., Voulgarakis, A., Kinney, P. L., Randerson, J. T., Shindell, D. T.,
7 Chen, Y., Faluvegi, G. (2013). El Niño and health risks from landscape fire emissions in
8 southeast Asia. Nat. Clim. Change, 3, 131-136.
- 9 Marsh, A., Miles, R. E. H., Rovelli, G., Cowling, A. G., Nandy, L., Dutcher, C. S., and Reid, J. P.
10 (2017). Influence of organic compound functionality on aerosol hygroscopicity: Dicarboxylic
11 acids, alkyl-substituents, sugars and amino acids. Atmos. Chem. Phys., 17, 5583-5599.
- 12 Massling, A., Leinert, S., Wiedensohler, A., Covert, D. (2007). Hygroscopic growth of sub-
13 micrometer and one-micrometer aerosol particles measured during ACE-Asia. Atmos. Chem.
14 Phys., 7, 3249-3259.
- 15 Massling, A., Wiedensohler, A., Busch, B., Neusüß, C., Quinn, P., Bates, T., and Covert, D.
16 (2003). Hygroscopic properties of different aerosol types over the Atlantic and Indian Oceans,
17 Atmos. Chem. Phys., 3, 1377-1397.
- 18 Massoli, P., Lambe, A. T., Ahern, A. T., Williams, L. R., Ehn, M., Mikkilä, J., Canagaratna, M.
19 R., Brune, W. H., Onasch, T. B., Jayne, J. T., Petäjä, T., Kulmala, M., Laaksonen, A., Kolb, C.
20 E., Davidovits, P., and Worsnop, D. R. (2010). Relationship between aerosol oxidation level and
21 hygroscopic properties of laboratory generated secondary organic aerosol (SOA) particles,
22 Geophys. Res. Lett., 37, L24801.
- 23 Mircea, M., Facchini, M. C., Decesari, S., Cavalli, F., Emblico, L., Fuzzi, S., Vestin, A., Rissler,
24 J., Swietlicki, E., Frank, G., Andreae, M. O., Maenhaut, W., Rudich, Y., and Artaxo, P. (2005).
25 Importance of the organic aerosol fraction for modeling aerosol hygroscopic growth and
26 activation: a case study in the Amazon Basin. Atmos. Chem. Phys., 5, 3111-3126.
- 27 Ng, N. L., Canagaratna, M. R., Jimenez, J. L., Chhabra, P. S., Seinfeld, J. H., and Worsnop, D. R.
28 (2011). Changes in organic aerosol composition with aging inferred from aerosol mass spectra.
29 Atmos. Chem. Phys., 11, 6465-6474.
- 30 Ng, N. L., Canagaratna, M. R., Zhang, Q., Jimenez, J. L., Tian, J., Ulbrich, I. M., Kroll, J. H.,
31 Docherty, K. S., Chhabra, P. S., Bahreini, R., Murphy, S. M., Seinfeld, J. H., Hildebrandt, L.,
32 Donahue, N. M., DeCarlo, P. F., Lanz, V. A., Prevot, A. S. H., Dinar, E., Rudich, Y., and
33 Worsnop, D. R. (2010). Organic aerosol components observed in Northern Hemispheric datasets
34 from Aerosol Mass Spectrometry, Atmos. Chem. Phys., 10, 4625-4641.
- 35 Ogawa, S., Setoguchi, Y., Kawana, K., Nakayama, T., Ikeda, Y., Sawada, Y., Matsumi, Y., and
36 Mochida, M. (2016). Hygroscopicity of aerosol particles and CCN activity of nearly
37 hydrophobic particles in the urban atmosphere over Japan during summer. J. Geophys. Res.
38 Atmos., 121, 7215-7234.
- 39 Paatero, P., and Tapper, U. (1994). Positive matrix factorization: A nonnegative factor model
40 with optimal utilization of error estimates of data values. Environmetrics, 5, 111-126.



- 1 Page, S. E., Siegert, F., Rieley, J. O., Boehm, H.-D. V., Jaya, A., Limin, S. (2002). The amount
2 of carbon released from peat and forest fires in Indonesia during 1997. *Nature*, 420, 61-65.
- 3 Page, S., Hoscilo, A., Langner, A., Tansey, K., Siegert, F., Limin, S., and Rieley, J. (2009).
4 Tropical peatland fires in Southeast Asia, in: *Tropical Fire Ecology: Climate Change, Land Use
5 and Ecosystem Dynamics*, edited by: Cochrane, M. A., Springer-Praxis, Heidelberg, Germany,
6 645 pp.
- 7 Park, K., Kittelson, D. B., Zachariah, M. R., and McMurry, P. H. (2004). Measurement of
8 inherent material density of nanoparticle agglomerates. *J. Nanopart. Res.*, 6, 267-272.
- 9 Peng, C., Chan, M. N., and Chan, C. K. (2001). The hygroscopic properties of dicarboxylic and
10 multifunctional acids: Measurements and UNIFAC predictions, *Environ. Sci. Technol.*, 35, 4495-
11 4501.
- 12 Petters, M. D., Carrico, C. M., Kreidenweis, S. M., Prenni, A. J., DeMott, P. J., Collett Jr., J. L.,
13 and Moosmuller, H. (2009). Cloud condensation nucleation activity of biomass burning aerosol.
14 *J. Geophys. Res. Atmos.*, 114, D22205.
- 15 Petters, M. D., and Kreidenweis, S. M. (2007). A single parameter representation of hygroscopic
16 growth and cloud condensation nucleus activity. *Atmos. Chem. Phys.*, 7, 1961-1971.
- 17 Petters, M. D., Kreidenweis, S. M., and Ziemann, P. J. (2016). Prediction of cloud condensation
18 nuclei activity for organic compounds using functional group contribution methods. *Geosci.
19 Model Dev.*, 9, 111-124.
- 20 Psichoudaki, M. and Pandis, S. N. (2013). Atmospheric aerosol water-soluble organic carbon
21 measurement: A theoretical analysis. *Environ. Sci. & Technol.*, 47, 9791-9798.
- 22 Reid, J. S., Hyer, E. J., Johnson, R. S., Holben, B. N., Yokelson, R. J., Zhang, J., Campbell, J. R.,
23 Christopher, S. A., Girolamo, L. D., Giglio, L., Holz, R. E., Kearney, C., Miettinen, J., Reid, E.
24 A., Turk, F. J., Wang, J., Xian, P., Zhao, G., Balasubramanian, R., Chew, B. N., Janjai, S.,
25 Lagrosas, N., Lestari, P., Lin, N.-H., Mahmud, M., Nguyen, A. X., Norris, B., Oanh, N. T. K.,
26 Oo, M., Salinas, S. V., Welton, E. J., and Liew, S. C. (2013). Observing and understanding the
27 Southeast Asian aerosol system by remote sensing: An initial review and analysis for the Seven
28 Southeast Asian Studies (7SEAS) program. *Atmos. Res.*, 122, 403-468.
- 29 Reid, J. S., Koppmann, R., Eck, T. F., and Eleuterio, D. P. (2005). A review of biomass burning
30 emissions part II: intensive physical properties of biomass burning particles. *Atmos. Chem. Phys.*,
31 5, 799-825.
- 32 Riipinen, I., Pierce, J. R., Yli-Juuti, T., Nieminen, T., Häkkinen, S., Ehn, M., Junninen, H.,
33 Lehtipalo, K., Petäjä, T., Slowik, J., Chang, R., Shantz, N. C., Abbatt, J., Leaitch, W. R.,
34 Kerminen, V. M., Worsnop, D. R., Pandis, S. N., Donahue, N. M., and Kulmala, M. (2011).
35 Organic condensation: a vital link connecting aerosol formation to cloud condensation nuclei
36 (CCN) concentrations. *Atmos. Chem. Phys.*, 11, 3865-3878.
- 37 Riipinen, I., Rastak, N., Pandis, S. N. (2015). Connecting the solubility and CCN activation of
38 complex organic aerosols: a theoretical study using solubility distributions. *Atmos. Chem. Phys.*,
39 15, 6305-6322.



- 1 Robinson, A. L., Donahue, N. M., Shrivastava, M. K., Weitkamp, E. A., Sage, A. M., Grieshop,
2 A. P., Lane, T. E., Pierce, J. R., and Pandis, S. N. (2007). Rethinking organic aerosols:
3 Semivolatile emissions and photochemical aging, *Science*, 315, 1259-1262.
- 4 Rose, D., Nowak, A., Achtert, P., Wiedensohler, A., Hu, M., Shao, M., Zhang, Y., Andreae, M.
5 O., and Pöschl, U. (2010). Cloud condensation nuclei in polluted air and biomass burning smoke
6 near the mega-city Guangzhou, China – Part 1: Size-resolved measurements and implications for
7 the modeling of aerosol particle hygroscopicity and CCN activity. *Atmos. Chem. Phys.*, 10,
8 3365-3383.
- 9 Rosenfeld, D. (1999). TRMM observed first direct evidence of smoke from forest fires inhibiting
10 rainfall. *Geophys. Res. Lett.*, 26, 3105-3108.
- 11 Saxena, E., Hildemann, L. M., McMurry, E. H., and Seinfeld, J. H. (1995). Organics alter
12 hygroscopic behavior of atmospheric particles, *J. Geophys. Res.* 100, 18755-18770.
- 13 Spracklen, D. V., Reddington, C. L., and Gaveau, D. L. A. (2015). Industrial concessions, fires
14 and air pollution in Equatorial Asia. *Environ. Res. Lett.*, 10, 091001.
- 15 Stockwell, C. E., Jayarathne, T., Cochrane, M. A., Ryan, K. C., Putra, E. I., Saharjo, B. H.,
16 Nurhayati, A. D., Albar, I., Blake, D. R., Simpson, I. J., Stone, E. A., Yokelson, R. J. (2016).
17 Field measurements of trace gases and aerosols emitted by peat fires in Central Kalimantan,
18 Indonesia, during the 2015 El Niño. *Atmos. Chem. Phys.*, 16, 11711-11732.
- 19 Stokes, R. H., and Robinson, R. A. (1966): Interactions in aqueous nonelectrolyte solutions: I.
20 Solute-solvent equilibria. *J. Phys. Chem.*, 70, 2126-2130.
- 21 Suda, S. R., Petters, M. D., Yeh, G. K., Strollo, C., Matsunaga, A., Faulhaber, A., Ziemann, P. J.,
22 Prenni, A. J., Carrico, C. M., Sullivan, R. C., Kreidenweis, S. M. (2014). Influence of functional
23 groups on organic aerosol cloud condensation nucleus activity. *Environ. Sci. & Technol.*, 48,
24 10182-10190.
- 25 Topping, D. O., McFiggans, G. B., and Coe, H. (2005). A curved multicomponent aerosol
26 hygroscopicity model framework: Part 2 - Including organic compounds, *Atmos. Chem. Phys.*, 5,
27 1223-1242.
- 28 Turpin, B. J., Hering, S. V., and Huntzicker, J. J. (1994). Investigation of organic aerosol
29 sampling artifacts in the Los Angeles Basin, *Atmos. Environ.*, 28, 3061-3071.
- 30 Ulbrich, I. M., Canagaratna, M. R., Zhang, Q., Worsnop, D. R., Jimenez, J. L. (2009).
31 Interpretation of organic components from positive matrix factorization of aerosol mass
32 spectrometric data. *Atmos. Chem. Phys.*, 9, 2891-2918.
- 33 van der Werf, G.R., Randerson, J. T., Giglio, L., Collatz, G. J., Mu, M., Kasibhatla, P. S.,
34 Morton, D. C., DeFries, R. S., Jin, Y., van Leeuwen, T. T. (2010). Global fire emissions and the
35 contribution of deforestation, savanna, forest, agricultural, and peat fires (1997–2009). *Atmos.*
36 *Chem. Phys.*, 10, 11707-11735.
- 37 Winkler, P. M., Ortega, J., Karl, T., Cappellin, L., Friedli, H. R., Barsanti, K., McMurry, P. H.,
38 and Smith, J. N. (2012). Identification of the biogenic compounds responsible for size-dependent
39 nanoparticle growth, *Geophys. Res. Lett.*, 39, L20815.
- 40 World Health Organization. (2009). *Global Health Risks: Mortality and Burden of Disease*
41 *Attributable to Select Major Risks* (Geneva, Switzerland: World Health Organization). Available



- 1 at: http://www.who.int/healthinfo/global_burden_disease/GlobalHealthRisks_report_full.pdf, last
2 access: 24 April 2017.
- 3 Zhang, Q., Jimenez, J. L., Canagaratna, M. R., Allan, J. D., Coe, H., Ulbrich, I., Alfarra, M.,
4 Takami, A., Middlebrook, A. M., Sun, Y., Dzepina, K., Dunlea, E., Docherty, K., DeCarlo, P. F.,
5 D., S., Onasch, T. B., Jayne, J., Miyoshi, T., Shimo, A., Hatakeyama, S., Takegawa, N.,
6 Kondo, Y., Schneider, J., Drewnick, F., Borrmann, S., Weimer, S., Demerjian, K., Williams, P.,
7 Bower, K., Bahreini, R., Cottrell, L., Griffin, R. J., Rautiainen, J., Sun, J., Zhang, Y., and
8 Worsnop, D. (2007). Ubiquity and dominance of oxygenated species in organic aerosols in
9 anthropogenically-influenced Northern Hemisphere midlatitudes, *Geophys. Res. Lett.*, 34,
10 L13801.
- 11 Zhang, Q., Jimenez, J. L., Canagaratna, M. R., Ulbrich, I. M., Ng, N. L., Worsnop, D. R., Sun, Y.
12 (2011). Understanding atmospheric organic aerosols via factor analysis of aerosol mass
13 spectrometry: a review. *Anal. Bioanal. Chem.*, 401, 3045-3067.
- 14 Zhao, D. F., Buchholz, A., Kortner, B., Schlag, P., Rubach, F., Fuchs, H., Kiendler-Scharr, A.,
15 Tillmann, R., Wahner, A., Watne, Å K., Hallquist, M., Flores, J. M., Rudich, Y., Kristensen, K.,
16 Hansen, A. M. K., Glasius, M., Kourchev, I., Kalberer, M., Mentel, Th F. (2016). Cloud
17 condensation nuclei activity, droplet growth kinetics, and hygroscopicity of biogenic and
18 anthropogenic secondary organic aerosol (SOA). *Atmos. Chem. Phys.*, 16, 1105-1121.
- 19 Zhao, D. F., Buchholz, A., Kortner, B., Schlag, P., Rubach, F., Kiendler-Scharr, A., Tillmann, R.,
20 Wahner, A., Flores, J. M., Rudich, Y., Watne, Å K., Hallquist, M., Wildt, J., Mentel, Th F.
21 (2015). Size-dependent hygroscopicity parameter (κ) and chemical composition of secondary
22 organic cloud condensation nuclei. *Geophys. Res. Lett.*, 42, 10920-910928.
23



- 1 **Table 1.** Summary of the hygroscopicity parameters (κ) and material densities of different
2 chemical constituents utilized in the theoretical κ calculation with chemical data.

Chemical compounds	Hygroscopicity parameter, κ	Density (10^3 kg/m^3)
<i>SNA</i> [†]	0.59	1.77
<i>EC</i>	0	1.80
OOA	κ_{OOA} [*]	1.50
Bulk OA	κ_{org} [*]	1.40

- 3 [†] *SNA* includes all the sulfate, nitrate, and ammonium in submicron wildfire haze particles.
4 ^{*} κ_{OOA} and κ_{org} were derived from ambient water uptake measurements and chemical data, in
5 combination of the given parameters in Table 1, using the simplified algorithm introduced in
6 Sects. 3.3 and 3.2.



- 1 **Table 2.** Summary of averaged chemical characteristics of the 24 h $PM_{2.5}$ filter samples collected
 2 during 2015 haze events and the accordingly calculated mean κ results of organics ($RH = 85\%$).

Sampling date	Cl^- ($\mu\text{g}/\text{m}^3$)	NO_3^- ($\mu\text{g}/\text{m}^3$)	SO_4^{2-} ($\mu\text{g}/\text{m}^3$)	Na^+ ($\mu\text{g}/\text{m}^3$)	NH_4^+ ($\mu\text{g}/\text{m}^3$)	K^+ ($\mu\text{g}/\text{m}^3$)	Mg^{2+} ($\mu\text{g}/\text{m}^3$)	Ca^{2+} ($\mu\text{g}/\text{m}^3$)
Oct-14	0.64	2.40	10.21	0.20	4.93	0.62	0.05	0.55
Oct-15	0.38	1.72	10.51	0.18	4.63	0.60	0.03	0.50
Oct-16	0.27	1.62	9.01	0.25	4.03	0.48	0.08	0.65
Oct-19	0.65	2.39	15.90	0.20	7.99	0.58	0.03	0.41
Oct-20	0.24	1.09	10.22	0.31	4.33	0.51	0.05	0.48
Oct-21	0.19	0.83	7.95	0.23	3.15	0.51	0.08	0.52
Oct-22	0.23	0.80	9.71	0.29	3.78	0.38	0.08	0.50
Oct-23	0.56	2.65	15.92	0.18	9.13	0.70	0.005	0.25
Average	0.40	1.69	11.18	0.23	5.25	0.55	0.05	0.48

- 3 **Table 2. (continued)**

Sampling date	f_{inorg}^* (%)	$f_{SO_4^{2-}}$ (%)	f_{EC} (%)	$WSOC/OC$ (%)	Mean κ	Mean κ_{org}^\dagger ($D_\theta = 100\text{ nm}$)	Mean κ_{OOA}^\dagger
Oct-14	42.1	21.9	15.3	79.9	0.114	0.030	0.054
Oct-15	41.1	23.3	11.1	64.8	0.202	0.118	0.185
Oct-16	28.6	15.7	11.7	66.4	0.161	0.133	0.256
Oct-19	26.6	15.0	5.9	60.2	0.265	0.229	0.450
Oct-20	30.3	18.0	11.3	61.5	0.271	0.236	0.443
Oct-21	26.4	15.6	11.0	56.9	0.193	0.148	0.283



Oct-22	42.9	26.4	15.8	59.5	0.265	0.212	0.376
Oct-23	24.6	13.3	4.4	59.6	0.217	0.184	0.337
Average	30.5	17.2	10.8	63.6	0.211	0.161	0.298

1 * The subscript *inorg* stands for all the inorganic species; hence f_{inorg} is the mass fraction of
2 inorganic particles in the $PM_{2.5}$ filter sample. All the ionic data are provided with the mean mass
3 concentration ($\mu\text{g}/\text{m}^3$).

4 † The mean κ results of organics here were calculated with assuming 10.0 % elemental carbon
5 (*EC*) in total mass (see Sect.3.2).

6



- 1 **Table 3.** Derived mean κ values of organics with consideration of 10.0 % EC mass fraction in
2 total NR-PM₁, as well as the mean κ results for HTDMA measurements conducted within the
3 overlapped ToF-ACSM observation period of 10 – 24 October 2015 (i.e., κ_{HTDMA}).

	Mean κ (mean \pm SD)		
	Overall	Daytime	Nighttime
κ_{org}	0.157 \pm 0.108	0.200 \pm 0.104	0.103 \pm 0.086
κ_{OOA}	0.287 \pm 0.193	0.353 \pm 0.179	0.206 \pm 0.178
κ_{HTDMA}	0.207 \pm 0.093	0.247 \pm 0.096	0.160 \pm 0.063

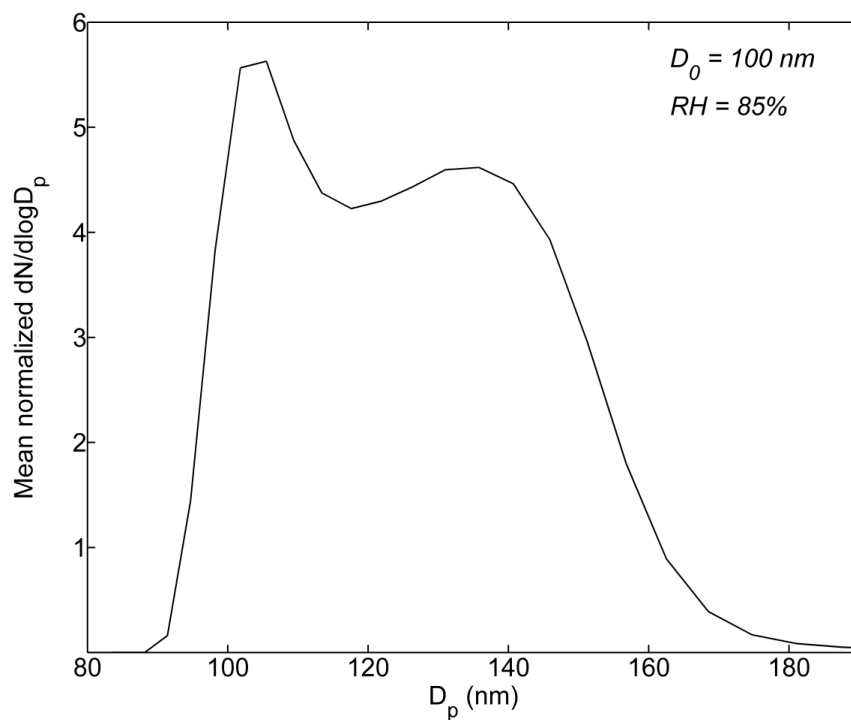
4



- 1 **Table 4.** The temporally mean number fraction (nf), volume-weighted mean diameter growth
- 2 factor (GF), and κ results (mean \pm SD) of 100 nm wildfire haze particles in the three different
- 3 hygroscopicity ranges at 85 % RH .

Hygroscopic mode	nf	GF	κ
Weakly ($g < 1.15$)	0.42 ± 0.18	1.05 ± 0.02	0.030 ± 0.013
Moderately ($1.15 \leq g < 1.27$)	0.18 ± 0.07	1.21 ± 0.01	0.151 ± 0.005
Highly ($1.27 \leq g < 1.85$)	0.40 ± 0.20	1.40 ± 0.05	0.343 ± 0.054
Bulk mean	n/a	1.25 ± 0.09	0.189 ± 0.087

- 4 n/a : not applicable.

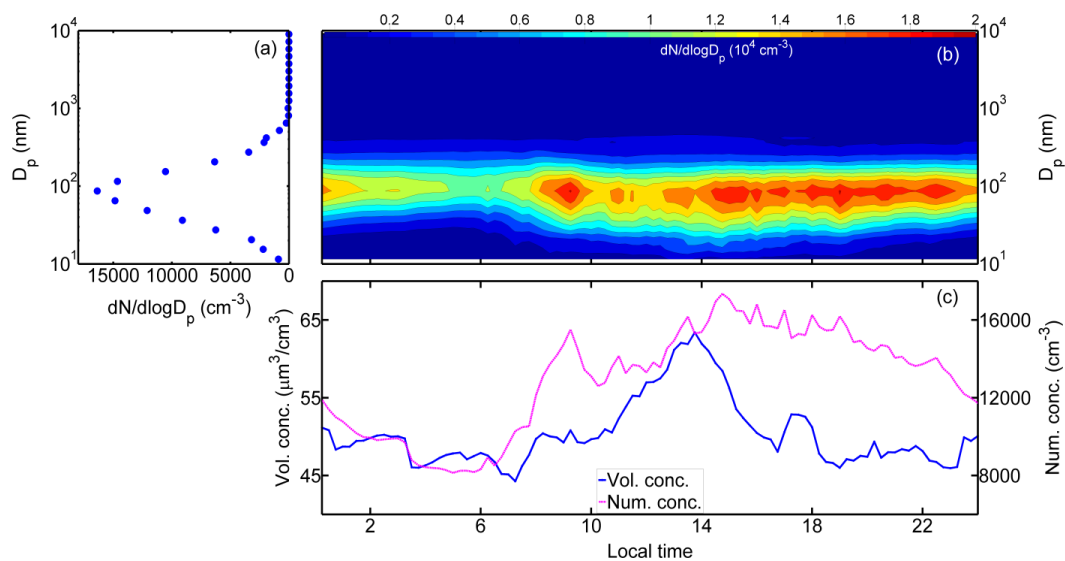


1

2 **Fig.1** Normalized particle number size distribution ($(dN/d\log D_p)/N$) after humidification

3 averaged over the whole haze observation period.

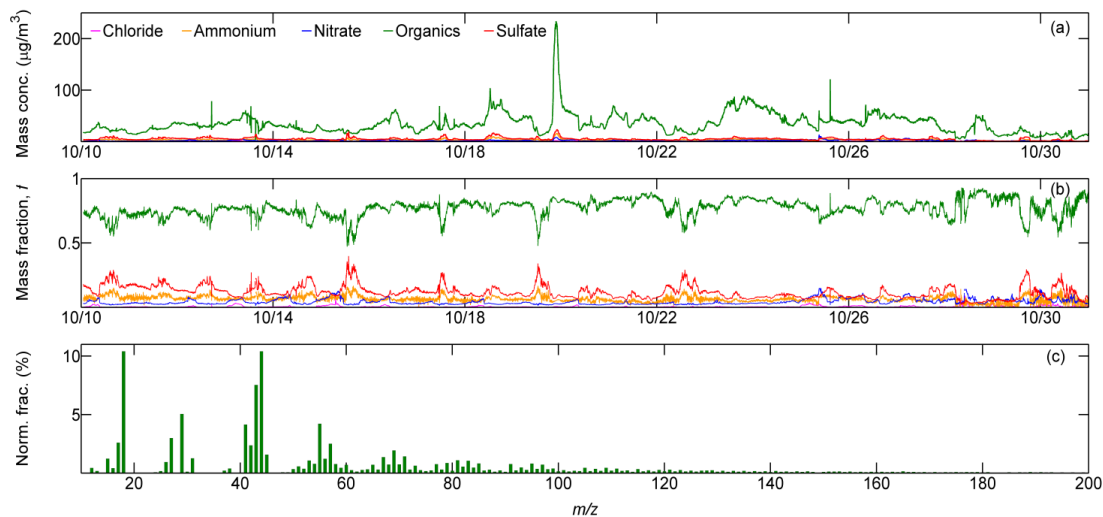
4



1

2 **Fig.2** (a) The mean normalized particle number size distribution ($dN/d\log D_p$, cm^{-3}) during the
3 ambient wildfire haze observations, as well as the mean diurnal variations of (b) normalized size
4 distribution, (c) number concentration (Num. conc., cm^{-3} , denoted by the magenta solid line) and
5 volume concentration (Vol. conc., $\mu\text{m}^3/\text{cm}^3$, as the blue line displayed) measured with
6 NanoScan-SMPS (11.5 – 365.2 nm) and OPS (419 nm – 10 μm) (local time, LT).

7 High aerosol loading was commonly observed during the transboundary wildfire haze.
8 Submicron particles in the size range of 30 – 200 nm dominated the total number concentration
9 of wildfire haze particles.

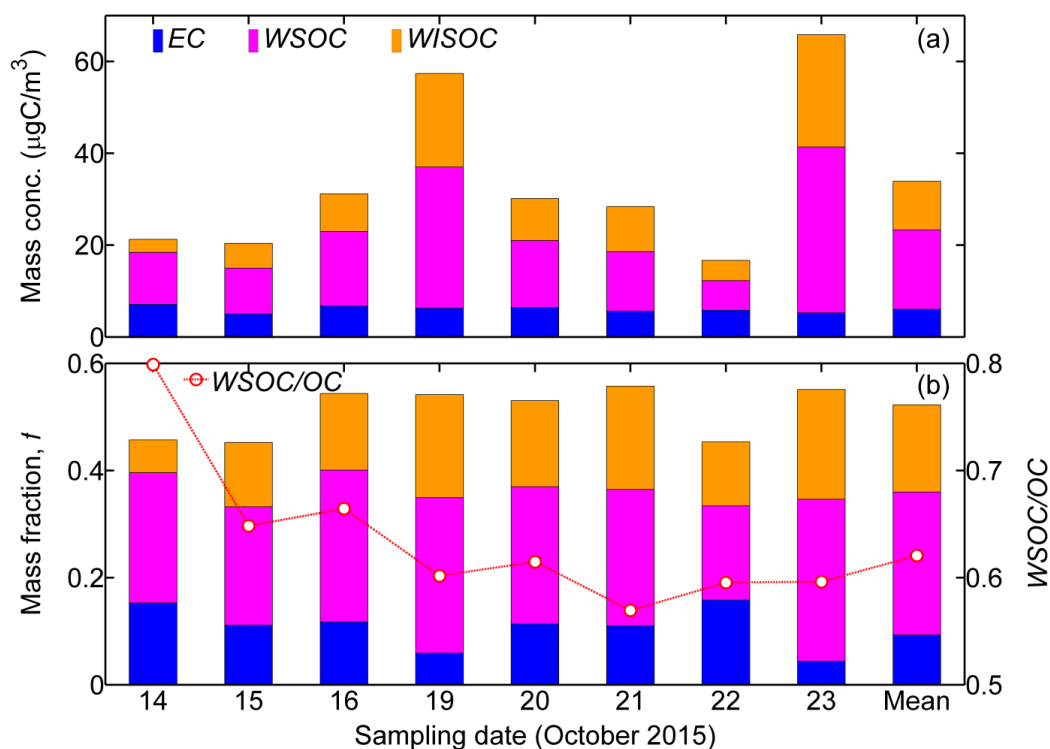


1

2 **Fig.3** Time series of (a) mass concentration (Mass conc., $\mu\text{g}/\text{m}^3$) and (b) corresponding mass
3 fraction, f , of the five specific chemical species in NR-PM₁ measured by ToF-ACSM (abscissa
4 shows the observation dates in October 2015, with the date format of Month/Day). (c)
5 Temporally averaged OA mass spectra for submicron wildfire haze particles, displayed with the
6 normalized ion fraction (Norm. frac., %) of each ion fragment.

7 Wildfire haze particles were predominantly composed of organics. Ion signals (m/z) from
8 oxygenated organics (e.g., m/z 43, 44) were prominent, while intensities of ions for hydrocarbon-
9 like organic compounds (e.g., m/z 41, 55, 57) and biomass burning tracers (e.g., m/z 60, 73) were
10 relatively less intense. See the text for details.

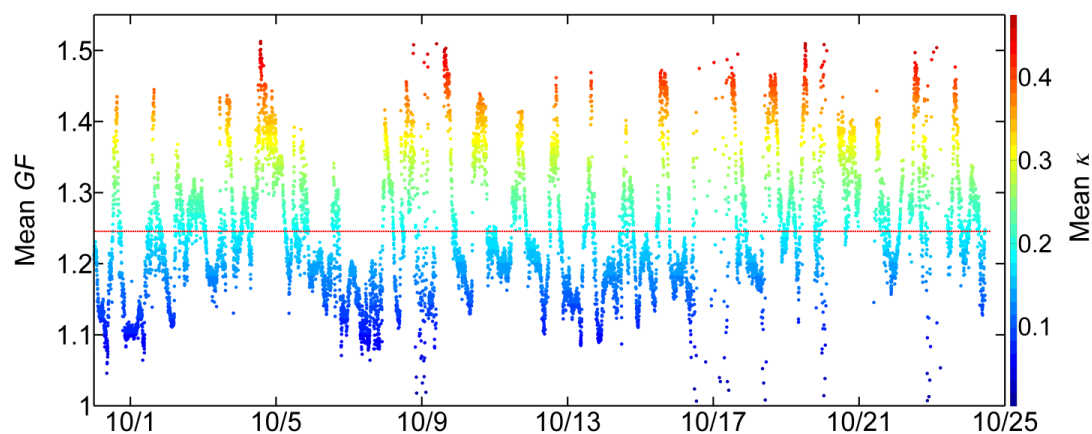
11



1

2 **Fig.4** (a) Mass concentration (Mass conc., $\mu\text{gC}/\text{m}^3$) and (b) corresponding mass fraction, f , of the
 3 carbon contents including *EC*, *WSOC*, and water-insoluble *OC* (*WISOC*) in $PM_{2.5}$ filter samples.
 4 The *WSOC/OC* ratio is also displayed by the scattered dots in panel (b). All the corresponding
 5 temporal mean results are shown as denoted by “Mean”.

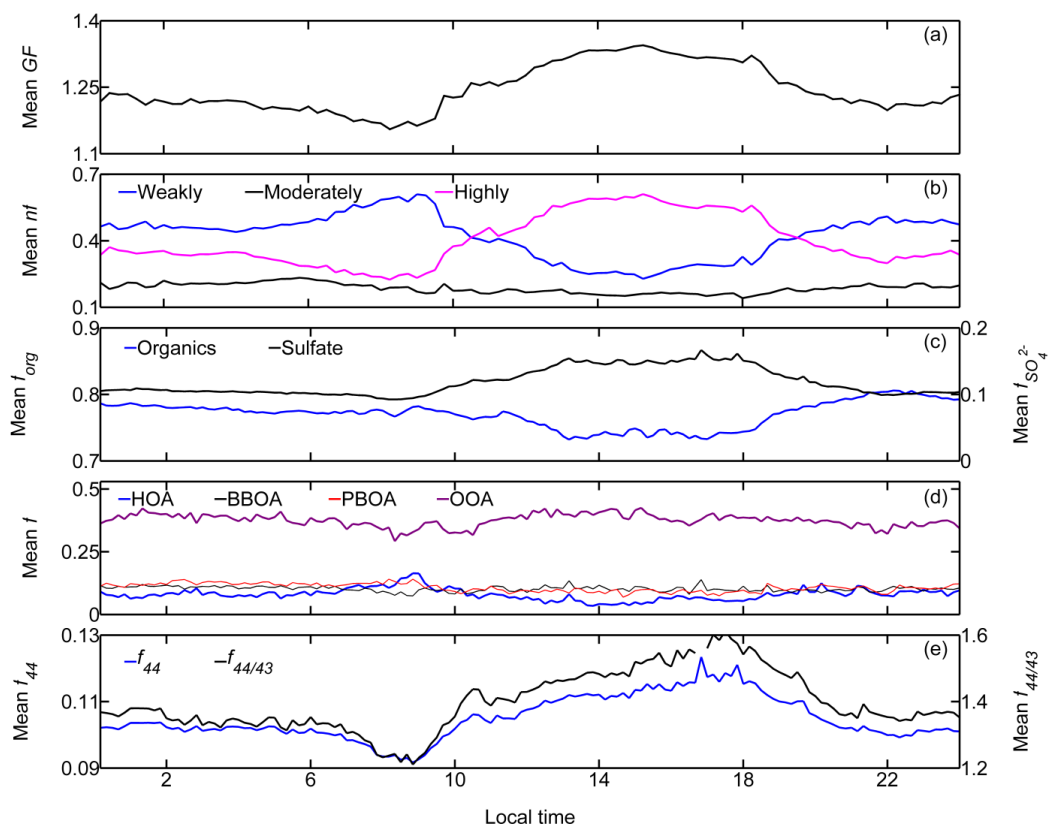
6 The *WSOC* fraction was exclusively higher than that of *WISOC* or *EC*, highlighting the
 7 dominance of *WSOC* in the carbon content of $PM_{2.5}$ filter samples. In general, the *EC* fraction
 8 fluctuates around 10.0 % of the total $PM_{2.5}$ mass.



1

2 **Fig.5** Time series of the volume-weighted mean particle diameter growth factor (GF) derived
3 from HTDMA measurements (date format: Month/Day, 2015), colored with the corresponding
4 mean hygroscopicity parameter, κ . The red dashed line stands for the temporal mean GF
5 averaged over the whole observation period.

6

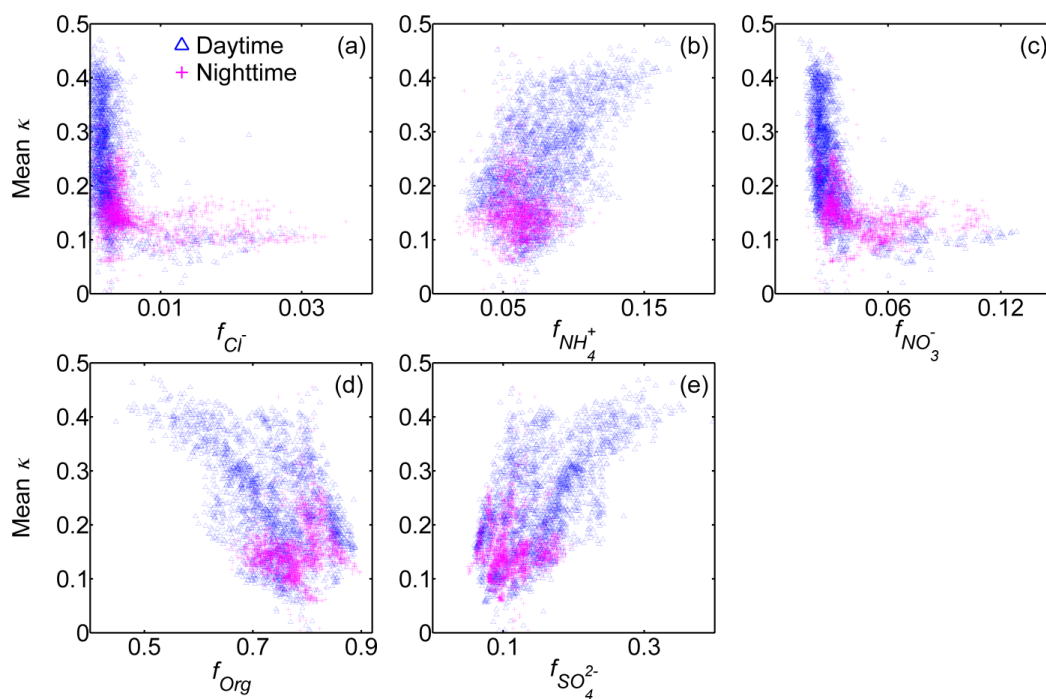


1

2 **Fig.6** Diurnal variations of (a) the mean GF , (b) number fraction (nf) of the three hygroscopic
 3 modes, (c) mass fraction of the two main components in NR-PM₁, i.e., organics (f_{org}) and sulfate
 4 ($f_{SO_4^{2-}}$), (d) mass fraction of ME2-resolved four OA factors in NR-PM₁ (i.e., f_{HOA} , f_{BBOA} , f_{PBOA} ,
 5 and f_{OOA}), and (e) mean f_{44} and $f_{44/43}$ of organics in NR-PM₁ (local time, LT).

6 Pronounced diurnal patterns were observed for the mean GF , number fractions of both weakly
 7 and highly hygroscopic modes, f_{44} , $f_{44/43}$, and mass fractions of organics and sulfate as well as
 8 HOA and OOA. nf_{highly} , $f_{SO_4^{2-}}$, f_{44} , $f_{44/43}$, and f_{OOA} show the similar variations to that of the mean
 9 GF , whereas contrary diurnal patterns are found for nf_{weakly} , f_{org} , and f_{HOA} .

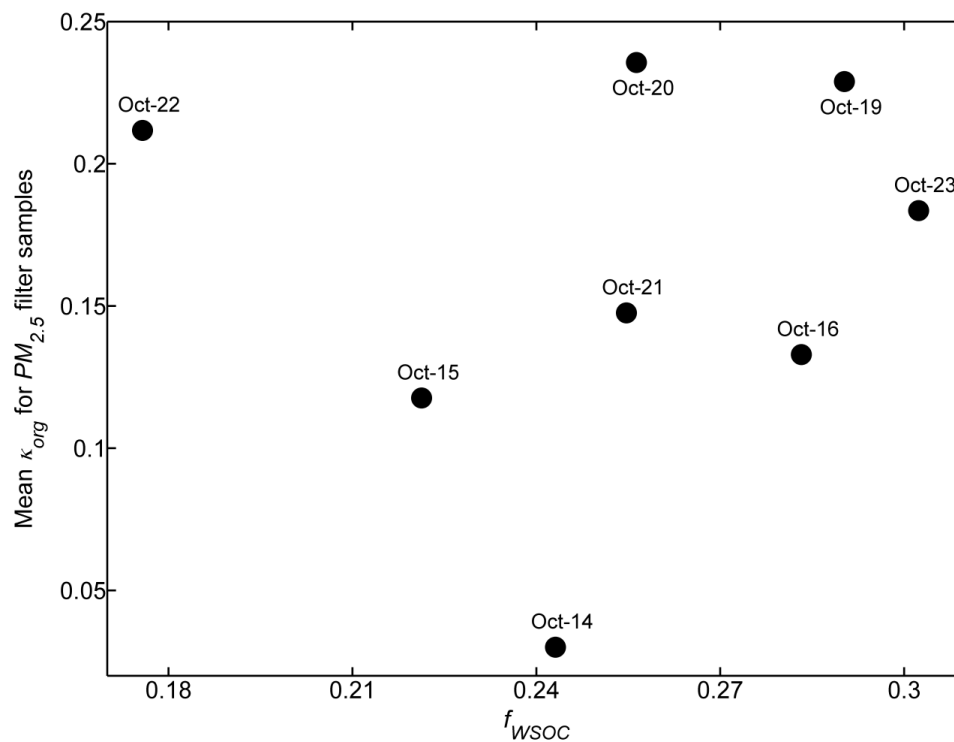
10



1

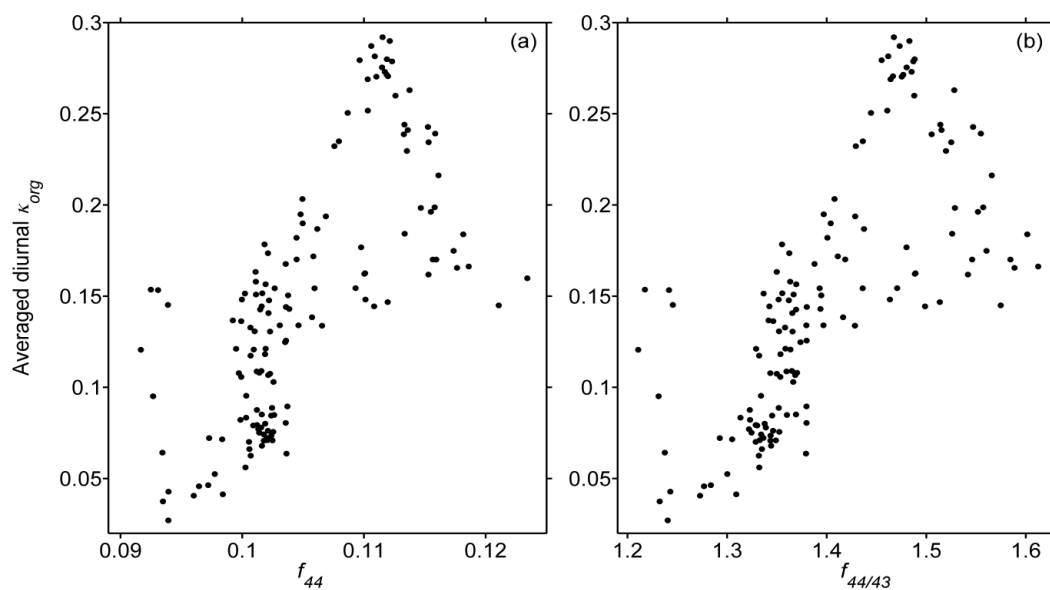
2 **Fig.7** Relationships between the mean κ results (100 nm) and mass fractions of the five non-
3 refractory chemical compositions in submicron wildfire haze particles.

4



1

2 **Fig.8** Correlation between the mean κ of organics (κ_{org} , with 10.0 % EC mass fraction taken into
3 consideration of the κ calculation) and the mean WSOC fraction (f_{WSOC}) of $PM_{2.5}$ filter samples.



1

- 2 **Fig.9** Relationships between the averaged diurnal κ_{org} results vs. (a) f_{44} and (b) $f_{44/43}$ in NR-PM₁
3 haze particles.